ChemElectroChem

Review
doi.org/10.1002/celc.202300408

Chemistry Europe
European Chemical Societies Publishing

www.chemelectrochem.org

Nanoparticles in Electrochemical Immunosensors – A Concept and Perspective

Francesca Polli,[a] Federica Simonetti,[a] Luca Surace,[a] Marco Agostini,[a] Gabriele Favero,[b] Franco Mazzei,*[a] and Rosaceleste Zumpano*[a]

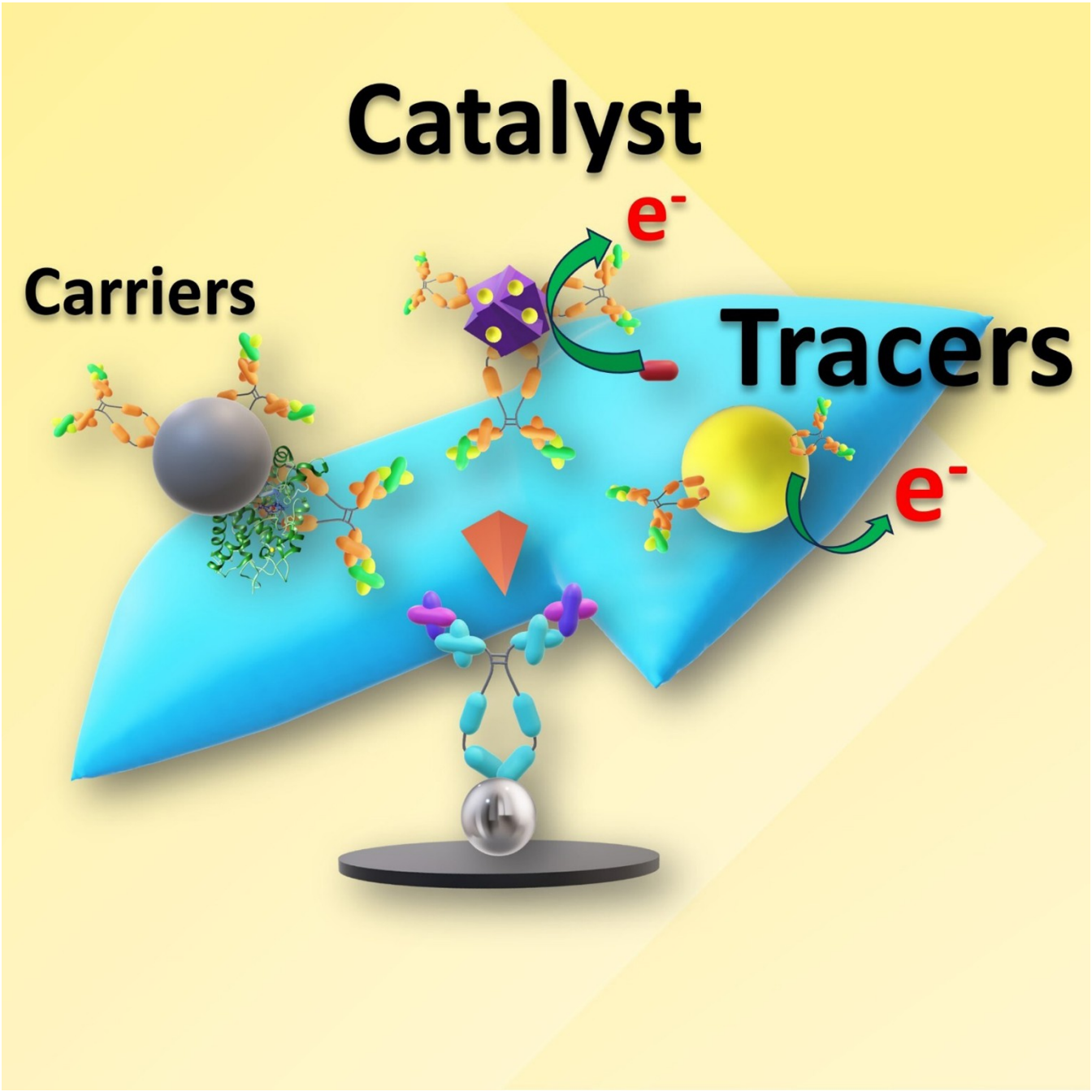

Nanoparticle-based electrochemical immunosensors are fascinating and promising screening systems that rely on the affinity binding between antibodies and antigens, allowing the specific detection of diverse types of targets (e.g., proteins, hormones, antibodies). The employment of nanoparticles in the realization of such devices dramatically improves the selectivity, sensitivity, and the transducer surface area for effectively immobilizing the bioreceptor or target molecules. During the last years, the nanoparticles design and fabrication was mainly focused on taking advantage from synergistic effects due to the coupling of different materials. In this review, we summarize the very recent advancements in this regard, with specific emphasis to nanoparticle syntheses procedures, antibody oriented immobilization strategies and transduction techniques. Moreover, the last trends and applications have been extensively discussed along with the remaining challenges and future perspectives.

1. Introduction

Integrating NMs and, more specifically, nanoparticles (NPs) in realizing electrochemical biosensors represented a crucial turning-point in the healthcare and medical diagnostic fields, environmental and food quality assessment.[1–3] One of the first applications of NP materials in biosensing dates back to the late 1990s and early 2000s, with the employment of Au colloids for labeling horseradish peroxidase (HRP) and improving the enzyme direct electron transfer (DET) at the electrode surface of an electrochemical biosensor for the detection of hydrogen peroxide.[4] Since then, the electrochemical sensing field has witnessed a rapid development of nanostructured materials, offering high performance and versatility for various applications.

Different kinds of NPs, such as metal, metal oxide, carbon, and polymer NPs, have been extensively investigated and utilized in developing electrochemical sensors and biosensors. NPs are widely used in biosensing applications due to their remarkable features, such as large surface area, high conductivity, electrocatalytic and electroactive properties, biocompatibility, and system miniaturization.[5] Among the electrochemical biosensors, those based on the affinity between antibodies (Abs) and related antigens (Ags) have gained ever more attention during the last years, as the very high specificity of the immune-recognition event.[6] Considering the electrochemical immunosensor set-up, the immobilization of immunoglobulins (Igs) onto the electrode surface enables the generation of an electrical signal resulting from the specific binding with the target analyte.[7] NPs offer various advantages for enhancing the performance of electrochemical immunosensors.[8] Different strategies have been developed to incorporate NPs into immunosensors, increasing their sensitivity, stability, and robustness. One of the most critical steps in this direction is the optimization of the recognition element immobilization onto the electrode surface, in which NPs play a pivotal role,[7] promoting the loading of Ab molecules and their optimal orientation at the transducer surface.[9] Additionally, various kinds of NPs can be integrated with other N-dimensional (ND) nanomaterials in nanocomposites, originating multifunctional, versatile, and hybrid sensing platforms.[10,11] At the same time, the synthesis and functionalization procedures to obtain stable and versatile NPs are a continuously evolving field of research to bring one-step and eco-friendly methods.[12–14] NPs with diverse shapes and sizes can be easily synthesized, being eco-friendly and free of chemical substances dangerous in the case of clinical and biological applications[15] (e.g., detection of clinically relevant biomolecules, such as cancer biomarkers or tumor cells).[7] Furthermore, minimizing interferences with the target signal in complex matrices (e.g., environmental and food samples)[16] becomes easier by involving NPs in the sample pre-treatment step.[17–20] Moreover, due to their extensively researched biocompatibility[21] and their crucial role in pandemic, a particular attention was given to the use of magnetic particles.[22,23] This review aims to evidence the recent advances in NP-based electrochemical immunosensors, giving theoretical elements for understanding the most influencing factors in immunosensor performance along with the latest innovations in Ab immobilization strategies, green synthesis, and detection techniques. We also discuss the challenges and future perspectives of this emerging field, which is currently the objective of continuous studies.

[a] *Dr. F. Polli, F. Simonetti, L. Surace, Dr. M. Agostini, Prof. F. Mazzei, Dr. R. Zumpano*
Department of Chemistry and Thechnology of Drugs
Sapienza, University of Rome
Piazzale Aldo Moro, 5, 00185 Rome (Italy)
E-mail: franco.mazzei@uniroma1.it
rosaceleste.zumpano@uniroma1.it
Homepage: https://web.uniroma1.it/dip_ctf/dipartimento/persone/docenti/professori-ordinari/mazzei-franco
https://research.uniroma1.it/researcher/1223117d1acea514309add25e737626a57cebac707e4-d5ef24f2210f

[b] *Prof. G. Favero*
Department of Environmental Biology
Sapienza, University of Rome
Piazzale Aldo Moro, 5, 00185 Rome (Italy)

2. NPs as a versatile tool in immunosensors design

Different NPs are employed in electrochemical immunosensors development, playing a dramatic role in enhancing such devices' sensitivity, conductivity, and stability. Specifically, NPs refer to nanostructures with all three dimensions smaller than 100 nm. However, this classification has been modified over the years, extending the size limit up to 500 nm and including in the NPs family those NMs with two dimensions smaller than 100 nm (e.g., nanotubes (NTs), nanowires (NWs), etc.).[24]

Examples are metallic and carbon NPs (MeNPs, CNPs), magnetic NPs (MNPs), quantum and carbon dots (QDs, CDs), multimetallic NPs (multiMeNPs), metal oxide NPs (MeONPs), carbon nanotubes (CNTs) and MeNWs.[25] NPs show characteristics of large surface area, high conductivity, electrocatalysis and electroactivity, and biocompatibility, strictly depending on their shape, material, and size.[26] Considering immunosensors design, NPs play different roles,[27] such as being optimal electrode materials enhancing the electron transfer (ET) and primary Ab (Ab_1) loading[28–30] (Figure 1). In this respect, the shape is a fundamental feature, as the presence of tips and edges in NPs dramatically increases the electrical conductivity, promoting

Francesca Polli graduated in Pharmaceutical Chemistry and Technology at the Sapienza University of Rome with a surface plasmon resonance study on antibodies orienting platform. During her Ph.D. in Pharmaceutical Sciences, she has focused in the development of high performance optical and electrochemical immunosensors for envoironmental and diagnostic purposes as well, for the design of new experimental plaforms for the site-direct immobilization of monoclonal antibodies or Fc receptors. She is currently working as post-doc researcher in the Department of Chemistry and Technology of Drugs (DCTF) in Sapienza University of Rome.

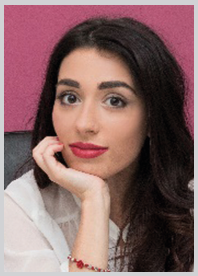

Federica Simonetti graduated from the University of Perugia, with a BA in chemistry and a MA in Physical Chemistry, with a dissertation on light scattering methods employed in the field of the analysis of complex systems. Later on, she achieved a Second Level Master at the University Sapienza of Rome in Forensic Analytical Methodologies. Now, she is a Ph.D. student in Pharmaceutical Science in the training group of Biosensors Lab, carrying out her research in environmental monitoring, risk assessment for water supply systems, development of smart environmental monitoring sensors and biosensors and the official analytical techniques for method validation.

Luca Surace received his master's degree in chemistry and Drug Technologies in 2022 from "La Sapienza" University of Rome. He is currently an international Ph.D. student in "Molecular design and characterization for the promotion of health and well-being: from drug to food" at the Biosensors Lab coordinated by prof. Franco Mazzei. His research is focused on the development of biosensors based on electrochemical methods to detection of biomarkers in diagnostic, food and environmental field.

Marco Agostini is graduated in industrial chemistry at Sapienza, University of Rome, BD and MD in December 2009 and October 2011 respectively. In November 2011 he started a Ph.D. in materials science at the same university, working in the group of Prof. Bruno Scrosati. From 2016 to 2020 he worked at the Chalmers University of Technology, and since 2022 he is a tenure track researcher at Sapienza, University of Rome. His current research topic is to develop new materials for applications in Li-ion batteries and he started research in electrochemical biosensors.

Gabriele Favero is Full Professor of Chemistry of the Environment and Cultural Heritage, he is Chairman of Didactic Board in Science and Technologies for the Conservation of Cultural Heritage at Sapienza University of Rome, and national representative for Graduation Classes in Science Applied to Cultural Heritage at the National Conference of Presidents and Directors of the University Courses of Science and Technology (con.Scienze). He is author of 130 papers in national and international journals and one patent in various fields with particular reference to electroanalytics and bioelectrochemistry, for sensors and biosensors development, and diagnostics of cultural heritage.

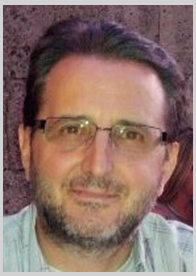

Franco Mazzei is Full Professor of Physical Chemistry at the Dept. of Chemistry and Drug Technologies, the University of Rome "La Sapienza", is responsible for the Biosensors Laboratory. He has published 128 papers in national and international scientific journals and five patents on various aspects of electrochemical and optical sensors and biosensors in national and international journals. He is involved in several research projects on developing nanotechnology-based electrochemical and optical biosensors in clinical, toxicological, and food fields, with grants from government and private institutions.

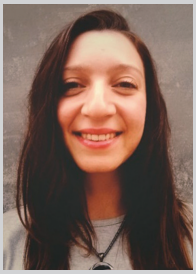

Rosaceleste Zumpano received her MD in Physical Chemistry and Ph.D. in Pharmaceutical Sciences from Sapienza University of Rome, specializing in light and X-ray scattering techniques and electrochemistry for the realization and characterization of enzymatic biosensors and immunosensors. Later, she held a two-years post-doc at the Department of Chemistry and Technology of Drugs (DCTF), Sapienza University of Rome, focusing her research on the synthesis of anisotropic metal nanoparticles and alloys, for developing highly sensitive sensors and biosensors in the field of environmental and diagnostic monitoring. Currently, she has a research fellowship funded by INAIL institute at DCTF, Sapienza University of Rome.

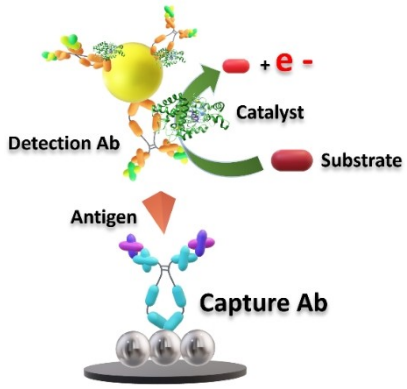

Figure 1. Typical asset for a sandwich electrochemical immunosensor. The capture Ab (in blue) is immobilized on the electrode, while the detection Abs are labeled with an enzyme (in green).

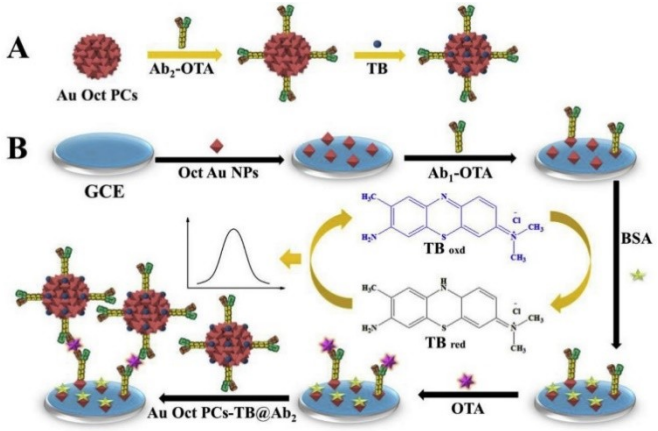

Figure 2. Figure of assembly of a sandwich electrochemical immunosensor described in the work of Zhang et al. with A) Nanomaterial batch Ab conjugation process and B) electrode modification. Reprinted with permission from Ref. [43]. Copyright 2018, Elsevier.

huge electrical fields in the proximity of crystal defects.[31] Moreover, the functionalization step for anisotropic or highly defective nanostructures is facilitated by their enhanced reactivity due to the exposed crystal facets ([110] and [100]).[32] In the latter case, the starting material is crucial too. For instance, in MeNPs, functionalization via spontaneous thiol-Me binding follows the reactivity order of Au > Cu > Ag.[33]

Other functions exploited by NPs in immunosensors development are electrocatalytic and electroactive tracers, nanocarriers,[34,35] where the nanostructure acts as secondary Ab (Ab_2) or capture Ab label, catalyzes specific electrochemical reactions and participates to detecting response or vectoring Ab_2 in indirect sandwich immunosensors.[36] Also, the NPs can be nanocarrier of several enzyme molecules such as HRP, allowing an intense signal amplification[37,38] when compared with the traditional Ab-HRP labeled systems.[39–41] The electrochemical device realized by Ma. and co-workers[42] is a fascinating example of NPs versatility in sandwich-type systems development. Gold triangular nanoprisms (AuTNPs) have been used as electrode material for improving ET and assisting the Ab_1 loading. At the same time, trimetallic yolk-shell Au@AgPt nanocubes (Au@AgPtYNCs) acted as Ab_2-nanocarriers for the detection of carcinoembryonic antigen (CEA) in tumor diagnosis and monitoring. Other examples of nanocarriers are gold colloidosomes plasmonic octahedrons (OctAuNPs) for ochratoxin A (OTA) detection,[43] as well as silver NPs (AgNPs) for dengue biomarker NS1 sensing[44] (Figure 2).

Palladium@Gold core-shell NPs (Pd@AuNPs) capped with N-(aminobutyl)-N-(ethylisoluminol) (ABEI) have been employed as nanocarriers for binding Ab_2 via Pd-N linkage.[45] Their further functionalization with ferrocene monocarboxylic acid (Fc-COOH) also made them electrocatalytic tracers simultaneously.

Pd at the nanoscale shows important catalytic activity towards H_2O_2 itself, being employable as a label inorganic catalyst in place of the more common horse radish peroxidase (HRP).[46]

Copper NPs (CuNPs) have been widely investigated for their cheapness than other noble metals,[47] showing great potential in producing customized electrodes. For instance, CuNPs can be used as electrochemical active labels[48] or electrode materials.[49] Platinum NPs (PtNPs), showing comparable conductivity to AuNPs, exhibit catalytic activity in chemical processes, including hydrogenation, electro-catalytic oxidation of formic acid or methanol, catalytic reduction of oxygen, and a few other redox reactions.[50] For this reason, PtNPs are optimal electrode materials,[51] nanocarriers[52] and catalytic amplifiers.[53] Carbon-based NPs are often coupled to several MeNPs and other materials to form "nanocomposites". Zhang et al.[54] used single-walled nanohorns (SWCNHs)-AgNPs composites as Ab_2 nanocarriers for ultrasensitive detection of sulphonamides. Graphene QDs (GQDs) have been employed for decorating zirconia (ZrO_2) nanoflowers (NFs) in realizing a label-free immunosensor for OTA detection in food matrices.[55] Similarly, multi-walled carbon nanotubes (MWCNTs) have been coupled with AuNPs in the realization of immunosensors for prostate-specific antigen (PSA) evaluation.[56]

Furthermore, several electrochemiluminescence (ECL) sensors have been developed over the years, by using nanoemitters[57] . The ECL activity of QDs have been widely studied such as Si, CdSe, PbS and other materials.[58] Specifically, QDs, luminophore-doped SiNPs showed higher solubility and low toxicity.[57] Metal nanoclusters (MeNCs) have also been reported to this aim. As an example, the protein-stabilized AgNCs conjugates signal can be properly amplified by employing TiO_2 and CNTs.[59] Furthermore, MOFs and COFs were also differently used.[57,58] Several MeONPs are employed accordingly to conventional MeNPs, such as TiO_2,[60] CeO_2[61] or Cu_2O.[62] In this regard, Fe_3O_4NPs represent a highly versatile category of NPs, satisfying the need for ET promotion, effective Ab immobilization and simplicity in separating the analyte simultaneously.[63] In particular, during COVID-19 pandemic, magnetic particles has been variously employed not just to develop rapid and portable diagnostic platform,[23,64] but also to predict its severity, through the detection of serum cytokines.[65,66] Between 2016–2022, MeONPs have been largely employed as electrode material, electroactive/electrocatalytic

tracers, and nanocarriers, and in sample pre-treatment procedures, deserving to be discussed in much more detail following (see paragraph 2.2).

2.1. NPs synthesis methods

Synthesis of NPs can follow two directions: top-down or bottom-up methods (Figure 3). The first approach uses bulk starting materials, progressively reducing the particle size to nanometric (nm) through physical, chemical, and mechanical processes. The second involves using atoms or molecules as starting material,[67] resulting in the best choice, since is low-cost, less time-consuming, and allows the possibility to tailor NPs size, shape, morphology, and composition. On the other hand, this approach often requires stabilizers, hazardous reagents, and high temperatures. Therefore, the research in this field is focused on optimizing these three parameters to improve the bottom-up synthesis to be more simple and green. Gold NPs (AuNPs), AgNPs, and gold/silver alloy NPs (AuAgNPs) stand out from the variety of NMs, due to their optoelectronic properties, shape tunability, biocompatibility, and easy bioconjugation. The most famous AuNPs and AgNPs synthesis protocols were developed by Turkevich and Brust, respectively[68,69] involving the reduction of Au and Ag salts by organic and inorganic reagents. The additional presence of stabilizers is generally required, avoiding possible aggregation due to the high-surface energy of these NMs.

Sodium citrate, ascorbate, sodium borohydride ($NaBH_4$), elemental hydrogen, polyols, Tollen's reagent, N, N-dimethylformamide (DMF), and poly (ethylene glycol)-block copolymers have been commonly used as reducing/capping agents to synthesize Au and Ag NPs of different size, shapes, morphology, and dimensions.[70] A variety of anisotropic nanostructures may be synthetized utilizing surfactants. In this regard, polyvinylpyrrolidone (PVP) and 2-14 cetyltrimethylammonium bromide (CTAB) were used in the synthesis of nanocubes and nanorods, respectively.[71,72] Also, high-hindrance polymeric compounds, such as poly (vinyl alcohol), poly (vinylpyrrolidone), poly (ethylene glycol), poly (methacrylic acid), and polymethylmethacrylate have been reported to be effective protective agents, allowing for highly-monodispersed-stable AuNPs.[8] In particular, employing polymers containing NH_2 group was demonstrated to be time-effective, condensing reduction and stabilization into just one step. While surfactants and long-organic molecules offer NPs morphology and shape tunability, they may represent a problem, consisting of a barrier between substrate and reactants and sometimes resulting cytotoxic. Recently, new synthetic approaches considered by a green-chemistry perspective have been developed, enabling high control over NPs morphology, shape, and monodispersity and allowing for the minimization of by-products, the utilization of nontoxic and green capping agents, the selection of environmentally benign solvents and sustainable synthesis conditions.[73,74] In this regard, these problems may be overpassed trough the choice of surfactant-free methods, which allow for anisotropic and "green" NPs synthesis.[75–78] As an example, gold nanostars (AuNSs) may be synthesized by a seed-mediated approach by adding $AgNO_3$ and ascorbic acid to the growth solution. Silver nitrate get instantaneously reduced to Ag^0 and used as seeds for anisotropic growth.[79] Polysaccharides, e.g., chitosan and sucrose, have recently been employed as protecting agents to synthesize "green" AuNPs. For instance, chitosan(CS)-AuNPs have been largely exploited for immunosensing as their biocompatibility, environmental safety, and easy-reliable synthesis.[80] Jiang et al.[81] reported that the CS-AuNPs could show peroxidase-like activity, facilitating the electrochemical reaction of H_2O_2 . Consequently, Patkin et al. synthetized CS-AuNPs by directly reducing $HAuCl_4$ precursor trough chitosan in solution.[82] The system was used as a label for the detection of CA125 oncological marker. Ultimately, if the goal is enhancing NP-loading capacity, dendrimers may be a very innovative solution.[83,84] PAMAM dendrimers are, by far, the hyperbranched polymers most exhaustively employed. As an example, Giannetto et al. proposed a sandwich immunosensors based on the electrodeposition of AuNPs on glassy carbon electrodes (GCEs), further functionalization with 2-aminoethanethiol and a covalently attached self-assembled monolayer of PAMAM G-1.5 dendrimer.[85] This platform allows for the Ab loading and was successfully validated also for serum samples. The chemical and physical properties derived from the synergistic and electronic effects between the metals make multiMeNPs promising for immunosensing applications.[86] The alloying with less-noble metals (e.g., Cu, Co, Ni) not only promotes the catalytic activity but also is convenient from an economic perspective.[87] As well explained by Loza et al.,[88] in the synthesis of bimetallic NPs, at least two metal precursors must be used. If both metal precursors are present in solution, their simoultaneous reduction may lead to alloyed NPs where two metals are present in a statistical mixture. In contrast, a

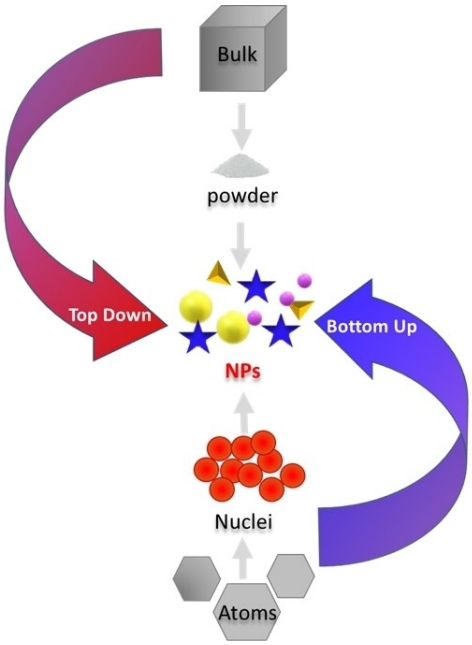

Figure 3. Scheme that depicts the different fabrication approaches *Bottom Up* and *Top Down* for NPs synthesis.

sequential reduction can lead to core-shell particles. Common synthetic methods for synthesizing multiMeNPs are the electrochemical and chemical methods.[89,90] Adopting the classification made by D. S. Idris and A. Roy,[91] the last ones could be grouped into two other large classes of methods: simultaneous reduction and successive reduction methods. Both methods are simple, fast and cheap, moreover, NPs properties (e.g., shape and dimensions) may be tuned by varying pH, temperature, or precursors' concentration. Some examples in the state-of-art of bimetallic NPs employed for immunosensors fabrication are AuAgNPs,[92] Pt-based NPs such as AuPt nano-chains and Au@Pt core/shell,[93,94] PdAuCu nanocrystals,[95] and trimetallic PdPtCuNPs,[96] $ZnFe_2O_4$-Ag/rGO nanocomposites,[97] PtCoCuPd alloyed tripods,[98] MoS_2@Cu_2O-Pt nanohybrids,[99] Au@Pd/Ag yolk-bimetallic shell NPs.[100] In 2018, Li et al. employed trimetallic PdPtCu nanospheres to detect PSA. These multimetallic nanospheres have been synthetized by a facile and reliable surfactant-direct strategy.[101] Although electrodeposition is a widespread practice for synthesizing these nanostructures, various green synthetic approaches have been developed in these years. For example, the synthesis procedure has synthetized AuAg bimetallic alloys by employing edible mushroom extract[102] or starch.[103] Another interesting example is the work of Wu et al.[97] ZnFe2O4-Ag/rGO nanocomposites have been synthesized through microwave-assisted (MW) preparation in mild conditions to develop a label-free immunosensor. MW is a break-through strategy very promising as a green method for NPs synthesis, allowing for rate enhancement, uniform heating, and high reproducibility.[104] In recent years, many signal amplification strategies have been developed in this field involving QDs. QDs, often described as "artificial atoms," can be classified differently based on their size and/or composition.[105] The choice of synthesis method can be a key factor in determining the properties of QDs. Top-down methods for their synthesis include laser ablation, electrochemical etching, liquid-phase exfoliation, electron beam lithography techniques, microwave irradiation, soft-template, pyrolysis, and wet-chemical reactions. Core-type QDS are very fluorescent materials composed of single-component materials, such as selenides, sulfides, or tellurides of metals like cadmium, lead, or zinc. Among them, Cadmium QD_S are very common. However, because of the cytotoxicity of Cadmium, great interest was demonstrated in Carbon QDS.[106] For their excellent chemical-physical properties, including quantum size effects, surface effects, and high electron density[107] these QDs have been employed in different fields and diagnostics. Karman et al., developed immunosensors based on Carbon dots, synthetized by a green hydrothermal reaction, starting from a citric acid solution and ethylenediamine.[108] Recently, GQDs have arisen as a new carbon nanomaterial showing hybrid features of graphene and carbon quantum dots.[109,110] Either top-down or bottom-up approaches can achieve the synthesis process of the GQDs with controllable size. In top-down methods, by the breaking down of two-dimensional (2D) graphene or graphene oxide (GO) sheets, carbon fibers, CNTs, or graphite 0D GQDs are formed. In contrast, in bottom-up processes, they are synthesized via stepwise reactions of small molecular precursors.[111] As a recent example, ZrO_2 Nanoflowers Decorated with Graphene Quantum Dots for Electrochemical Immunosensing have been synthesized by Pramod K. Gupta by using a one-pot hydrothermal approach.[110] As the literature shows, NPs for electrochemical immunosensing applications were also synthesized starting from semiconductor materials, such as Iron oxide, Copper oxide, and Titanium Oxide.[60,112–116] Among them, Iron oxide NPs are surely the most significant group.

2.2. A focus on MNP-based immunosensors

During the last decade, MNPs gained a great scientific interest in biomedical and diagnostic applications by virtue of the advantages associated with their magnetic properties and easy loading of proteins like enzymes and antibodies.[117,118] MNP, in its most basic form, comprises an inorganic magnetic core. It can often be coated by an additional layer (i.e., polymers, metals) to maximize its stability and reactivity with the external environment.[118–120] Thanks to their excellent biocompatibility and stability features, the most appropriate magnetic core among the different iron oxides to be described in immunosensor are maghemite (γ-Fe_2O_3) and magnetite (Fe_3O_4), which exhibit higher stability and higher saturation magnetization at room temperature.[121] Below 20 nm, the oxygen ions of those material arranged in a cubic close-packed lattice, with iron occuping the interstices.[122] At such small crystal sizes, a single magnetic domain is present and superparamagnetism is observed. As a result, these structures can be highly magnetized and will rapidly lose magnetization as soon as the magnetic field is removed. This feature makes them a valuable tool in different techniques like magnetic resonance imaging and hyperthermia therapy.[123] One of the main advantages of immunosensor development (Figure 4a) is their ability to be modified and purified easily by magnetic separation, avoiding any centrifugation step.[124] This feature has been explored for protein purification and to perform Ab-Ag interaction, as described in the work of Fabiani et al.[125] The immunocomplex is magnetically separated before it's cast on the electrode reducing the fabrication time and avoiding issues due to a direct interaction between the electrode surface and real matrices (i.e., non-specific adsorption). Furthermore, they can be easily drop-casted on electrodes with the help of magnetic support, preventing any material loss and without being affected by the "coffee ring effect".[126] However, the use of MNPs is not limited to magnetic separation. They can also be employed to increase the electrode *surface-to-volume* ratio[127,128] and – thanks to their magnetic properties – to improve the electrochemical signal by facilitating ET[127,129,130] when applied to Metal Organic Framework (MOF)[129] or other nanostructures. Wang et al.[130] used MNPs to decorate a graphene nanocomposite (TB-Au-Fe3O4-rGO) to magnify the electrochemical signal of the redox mediator toluidine blue. This work loaded the Ab on AuNPs and then drop-casted on the Fe_3O_4/rGO composite. The Fe_3O_4 roles of signal promotion and of sensing area increasing confers to this set up an extremely wide linear range from 1.0×10^{-5} ng/mL to 10.0 ng/mL and a LOD of 2.7 fg/

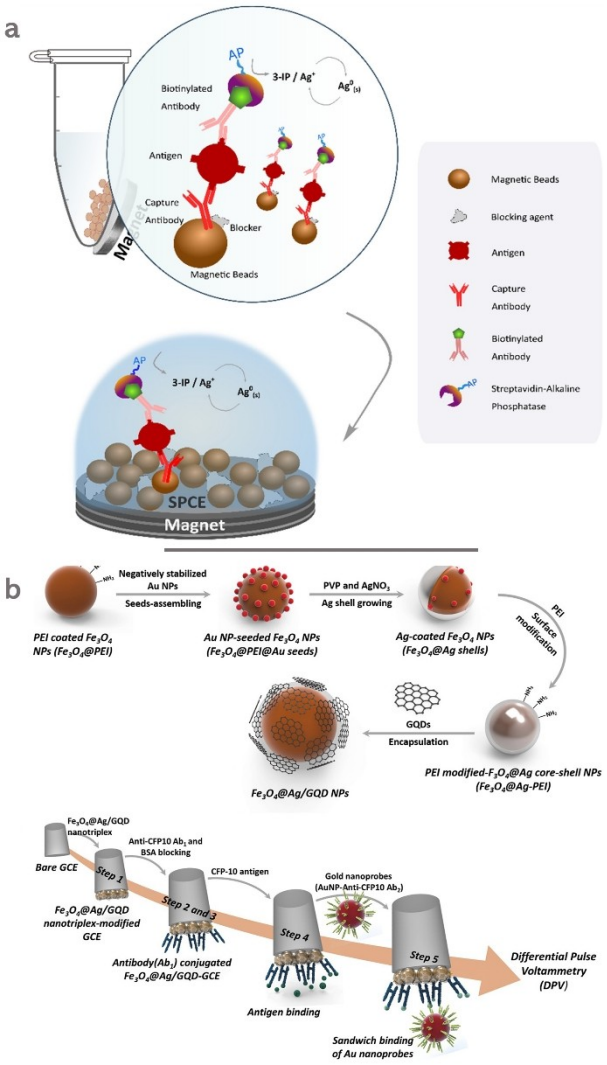

Figure 4. a) Example of magnetic-assisted procedures of purification and dropcasting in the work of Freitas et al. Reprinted with permission from Ref. [124]. Copyright 2020, Elsevier. b) Scheme of assembly described in the work of Tufa et al. where is reported the nanomaterial modification with Ag coated MNPs (up) and their employment in the immunoassay (down). Reprinted with permission from Ref. [127]. Copyright 2018, Elsevier.

mL for the detection of alpha-fetoprotein, paving the way to potential applications in the clinical diagnosis of other tumor markers. A similar use of this nanomaterial was adopted by Shamsazar et al.[131] in 2021, were Fe_3O_4NPs with unique properties for signal amplification have been synthesized. The capture antibodies were anchored to MWCNT-COOH groups to perform a sandwich-like immunoassay, while the detection antibodies were labeled with Horseradish Peroxidase (HRP). In the presence of H_2O_2, the enzyme-catalyzed its reaction, and the signal was strongly amplified by the Fe_3O_4 modification and proportional to the antigen content. This work exhibits a LOD 0.39 pg/mL and a wide linear range from 2.5 pg/mL to 100 ng/mL. Both the MNPs oxidation in air, and their tendency to aggregate in clusters, can be reduced by their encapsulation in charged molecules, polymers, or metallic shells. An impenetrable surface layer is thus formed around the particle, enhancing its stability over time. In particular, it is possible to synthesize water-soluble MNPs for biological applications by adding amino acids, citric acid, vitamins, and cyclodextrins in the reaction process.[119,132] For instance, poly carboxylic acid or polyamines often offers great stability as a capping agent by interacting with iron cations on the surface of MNPs. At the same time, uncoordinated groups contribute to stabilizing the dispersion by electrostatic repulsion. Otherwise, the metal coating allows the coupling of the physicochemical properties of the two materials in one nanostructure. As a result, metallic Core-shell MNPs,[132–134] have lately become very popular in immunosensor development as an effective way to stabilize magnetite and maghemite cores while leading an electrochemical signal amplification. A silver shell was synthetized by Ref. [127] to enhance the electrical conductivity of a nanotriplex-modified GCE (Figure 4b). Graphene-QDs increase the capture Ab loading on the electrode surface, while the detection antibodies are anchored on AuNPs. Subsequently, the quantification is obtained by monitoring the current given by the Au redox process released directly from the NP-Ab conjugate. This approach allows a LOD of 0.33 ng/mL and confers an excellent selectivity to pathogenic bacteria detection to the platform. However, gold is probably the most investigated material for MNPs coverage in immunosensing because it allows[135,136] to be easily functionalized with thiol groups, preparing NPs to be coupled with proteins.[137] This feature allows MNPs to be employed as Ab binding platforms by performing both batch and *layer-by-layer* modification. This feature has been exploited in several works.[138,139] For instance, we recently reported a new sensitive label-free electrochemical immunosensor to detect Vitamin D3 (25-OHD_3) in untreated serum samples. The sensing platform was realized by Au@MNPs functionalization with different thiols to improve the capture Ab immobilization. With this setup, we achieved one of the best performances in terms of sensibility and reproducibility among the validated 25-OHD_3 immunosensors (LOD of 2.4 ng mL^{-1}). These findings and the excellent agreement with the reference method suggest its potential use as a POCT to monitor hypovitaminosis 25-OHD_3 levels.

3. Antibody immobilization strategies on NPs

Numerous biotransducer immobilization strategies have been developed and reported to improve the conjugation of NPs.[140] In contrast to what has been described for solid support, NPs can be conjugated in batches and "layer by layer" after being cast on the electrode surface. Besides the type of functionalization, this step is particularly relevant in the case of antibodies, whose activity is strictly connected to their orientation on the electrode surface.[141–143] Nowadays, the main methods involve physical adsorption, covalent coupling, affinity (i.e., biotin/avidin system), direct immobilization of Fab fragments, and adsorption onto orienting molecules and proteins.[144] Generally, the chemical immobilization of antibodies on the sensor surface occurs at a random level, where antibodies are bound with the same probability in each of the four statistically relevant

configurations: *side on, lying on, head on*, and *end on*,[145–147] see Figure 5. This results in a lowered amount of Ab interacting with antigen, hence a decreased sensitivity). To solve this problem, several site-direct immobilization procedures have been developed, i.e., involving the use of an artificial linker[148,149] controlling the dipolar momentum, ionic exchanger, and the *Fc*'s N-glycan targeting through lectins and boronic acid.[142,150,151]

3.1. Physical adsorption

To date, physical adsorption of antibodies is one of the most easily implementable methods. This technique is the basis of ELISA (enzyme-linked immunosorbent assay)[152] and involves establishing hydrophilic or hydrophobic interactions with the electrode surface. These interactions allow using solid mediums of different typologies, such as polystyrene, silicone, nitrocellulose, or even metal surfaces.[153,154] However, the limitation of this technique lies in the adsorption process chosen for immobilization. Besides providing no control over the biotransducer's orientation, so far, showed other drawbacks, such as protein denaturation. Although by carefully modulate the envoiroment, protein stability can be improved, the limits on

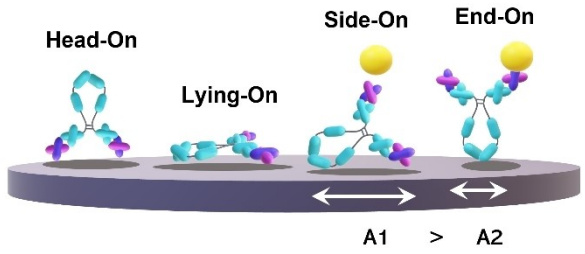

Figure 5. Ab orientation on sensor surfaces Different Ab orientations on the sensor surface. Vertical configurations (*head-on* and *end-on*) occupy a smaller surface area than horizontal configurations (*lying-on* and *side-on*), thus leading to a higher packing density.

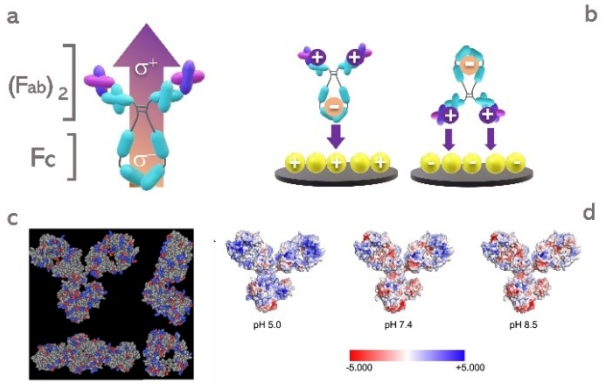

Figure 6. IgG_1 dipole moment direction a) and b) different orientations on positive and negative charged NPs. c) Acidic and basic residues distribution in Fab and Fc Ab fragments (marked in red and blue respectively). Reprinted with permission from Ref. [160]. Copyright 2019, American Chemical Society. d) Electrostatic map potential calculated for IgG1 Ab at pH 5–8.5 with PyMol 3.3 (PDB code: 1IGY). Reprinted with permission from Ref. [161]. Copyright 2022, Elsevier.

physical adsorption relies in the obtainment of a good reproducibility and in the absence of a control over the biotransducer orientation.[147,155] On the other hand, covalent conjugation allows to achieve a better Ab immobilization in terms of long-term stability of the coupled platform.[155] For many reasons, direct covalent cross-linking antibodies on the reactive surface have been more widely used in the state-of-art. However, the physical orientation can be influenced by the charges present at the surface of the electrode. As shown by Bujis et al., the positive, negative, and hydrophobic surfaces can drive the Ab orientation, depending on the isoelectric point, the dipole moment of the IgG, and the immobilization pHs. As shown in Figure 6,[145,156,157] basic residues are more abundant in the Fab region, leading to a dipole moment pointing from the Fc to the Fab.

Another possibility of physically immobilizing or labeling Ab in electrochemical immunosensors development is the realization of nano-bioconjugates, where the biological recognition element is physically conjugated to NPs or NMs in general.[158] On the contrary, the direct adsorption onto macroscopic surfaces, where the eventual denaturation process results more severe, and the physical conjugation of Ab to NMs is known for better preserving the protein's biological activity. When the adsorbent material approaches the protein size, its available area in contact with the biomolecule is reduced, providing for decreasing the interaction forces intensity.[159]

In addition, when the Ab is adsorbed onto flat surface macroscopic materials, the rise of protein-protein lateral interactions must be considered, causing cooperative or anti-cooperative effects affecting the protein biological activity as well.[162] Conversely, when NMs are employed, the curvature increase limits the lateral interactions, exposing more of the Ab to the solution and promoting a better sensitivity. Hence, the physisorption to noble MeNPs, alloys, MultiMeNPs, MeONPs is a common practice for labeling Abs in sandwich-type immunosensors. Core-shell Pd@PtNPs have been conjugated to Ab, obtaining sensitive electrocatalytic tracers for a-fetoprotein detection in human serum;[163] similarly, Ab_2-AuNPs bioconjugates have been used for enhancing the electrochemical signal in breast cancer patient HER-1 and HER-2 immunosensing.[164] In practice, the physical bioconjugation takes place as follows: i) electrostatic interaction between the negatively/positively charged NP surface or capping agents and the oppositely charged portion of the Ab; ii) hydrogen bonding promoted by NPs water or capping molecules towards the Ab amino acids residues; iii) hydrophobic interaction and/or cysteine adsorption at the NPs surface.[165] The i) and ii) belong to the real first stage of the overall mechanism, where the Ab is rapidly adsorbed onto the NPs surface. The iii) occurs later, during an internal reorganization step, which is also responsible for the eventual conformational changes in the protein. This behavior is likely the same at carbon-based nanomaterial interfaces[166] and related composites, only changing in terms of the intensity of the specific forces involved in the physisorption process. In general, NMs exposing hydrophilic surfaces mainly promote hydrogen bonding between the protein and surface water molecules, decreasing the intermolecular hydrophobic forces

responsible for stabilizing the protein structural motifs. This phenomenon is often the cause of protein denaturation. Meanwhile, NMs exposing hydrophobic surfaces promote stronger hydrophobic interactions, leading to additional intramolecular hydrogen bonding and protein transition to non-native conformations, with increased or decreased biological activity.[167] Therefore, a combination of different NMs in producing nanocomposites represents an optimal solution for obtaining synergistic effects in Ab physical adsorption and immunosensing performance, mitigating the risk of extreme denaturation phenomena. Detection Ab labeled single-walled carbon nanohorns (SWCNHs)/thionine(thi)/AuNPs has been realized, working as electroactive tracers for the detection of carcinoembryonic antigen,[168] or polyvinylpyrrolidone-capped AgNPs/MWCNTs were conjugated with TIR2 Abs to determine aspartame in food samples.[169] The physical bioconjugation in electrochemical immunosensor fabrication can be achieved both in solution or following a layer-by-layer procedure. As examples, AuNPs-Ab or AgNPs-Ab bioconjugates have been prepared in solution, realizing Ab-tagged bio probes for assemblingandwich-type electrochemical immunosensors.[170,171] Conversely, AuNRs-Ab or ZnO-CuO-Ab bioconjugates have been prepared by incubating the Ab solution onto electrodes already modified with these NMs, promoting the Ab physical adsorption through a layer-by-layer method.[172,173]

3.2. Covalent coupling

Antibody coupling with nanomaterial is one of the crucial step influencing immunosensor sensitivity. To this reason we have summarized in Figure 7, several immobilization techniques most described in literature. Amide coupling is one of the most widely used routes for protein immobilization to provide good stability and reproducibility on the process compared to physical adsorption.[147,155] In this technique, the electrode's surface is firstly modified with carboxylic groups using various strategies (e.g., self-assembled monolayers, polymer). Next, in a mildly acidic environment, -COOH groups are activated using EDC/NHS, see Figure 7a. This coupling reagent can prepare the carboxyl groups to host the nucleophilic attack of the protein amino moieties.[174] The antibodies' exposed ε – aminic lysine residues can now react with the activated groups of the chemical matrix to form a stable covalent amide bond. Despite the high reproducibility and stability given to the biotransducer immobilization, this methodology does not allow any orientation of the protein because it targets nucleophilic moieties that are heterogeneously distributed over the protein and therefore has no efficiency in avoiding the hindering of the *Fab*.[175] However, some optimization can limit EDC/NHS random orientation and involves a fine pH regulation. Mild acidic conditions have been reported to mitigate the attraction between the *Fab* fragment and the negative COO-electrode surface,[174] rich in basic residues. This finding was described by Lou et al. in 2019, who aim to improve the Ab orientation onto polystyrene nanospheres by pH optimization of EDC/NHS reaction.[160] By carefully evaluating the Ab and the NPs charge

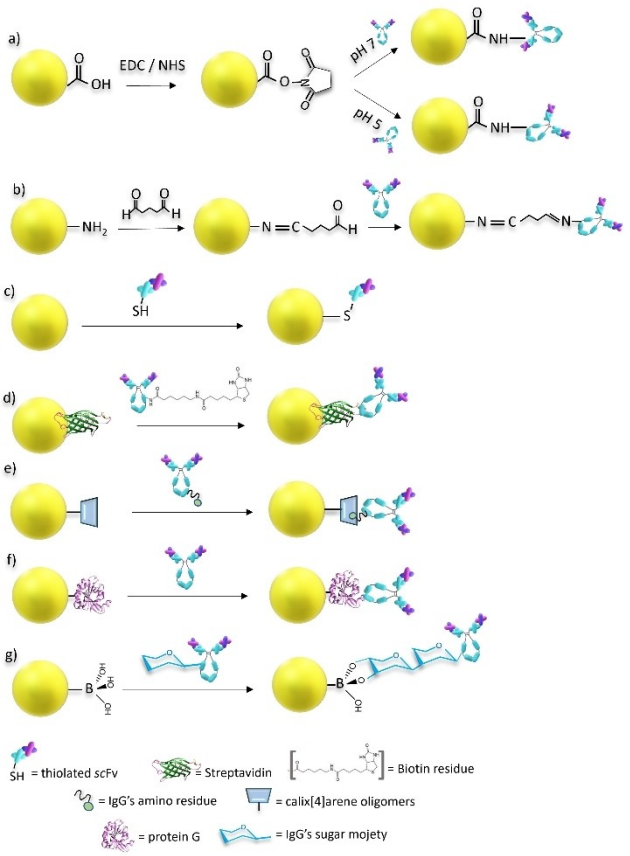

Figure 7. Ab Immobilization routes a) EDC/NHS cross-linking, b) glutaraldehyde reaction, immobilization, c) scFv-SH direct immobilization on Au d) Streptavidin-biotin immobilization protein G interaction e), calix[4]arene adsorption f) and boronic acid interaction g).

distributions, a control over orientation was achieved. For instance, a slightly acidic environment was able to reduce the cross-linker reaction rate, allowing the Ab to approach in the *end-on* configuration to the surface before being covalently immobilized.

Another commonly used technique for enzyme and Ab immobilization is using glutaraldehyde, to activate supports containing primary amino groups.[176,177] One option in immobilizing proteins via glutaraldehyde chemistry is to absorb the protein on aminic substrate previously and then, to mildly threat it with glutaraldehyde to allow a tight cross-linking by using a glutaraldehyde/amino moieties ratio around 1:1.[178,179]

However, this might not be a suitable protocol for what concern Ab because a high reticulation may limit the availability of the protein to the analyte. A more efficient route in Ab immobilization involves a different set up of glutaraldehyde cross-linking when a simple and ordered platform is required. These supports are developed by a first glutaraldehyde treatment of amino-modified surface with in a 1:2 ratio of glutaraldehyde/amino groups. This route confers to the platform a higher sensing surface without reducing the availability of the Fab to the antigen.[178]

3.3. Site-direct approach

Several strategies have been developed to limit the arbitrary orientation presented during antibody immobilization for sensing applications. One of the first was widely investigated between 2005 and015.[180] It is based on Fab fragments directly coupling on NPs and has been reported to improve the sensitivity up to 20-fold over standard amine coupling. It is based on an Ab pre-treatment with reducing agents - or using UV light - to break the disulfuric bridges hence attaching the fragment directly to the gold substrate through its -SH groups. However, they require time and effort for the Ab processing before immobilization, such as enzymatic digestion to obtain IgG fragments (Fab, Fc, etc.) or disulfide bond reduction.[180,181] These approaches can have a negative impact on the biological activity and affinity of the biomolecule if the experimental conditions are not carefully controlled. Therefore, this approach has been gradually replaced with the so-called "*scFv*" (single chain variable fragments) that is directly obtained by genetic engineering, thus avoiding protein manipulation. In this regard, Fadhilah et al.[182] (Figure 8) obtained thiolated scFv by adding a cysteine gene in the protein-coding, to allow their direct immobilization on gold NPs via S-Au formation. The EIS immunosensor was able to detect SARS-CoV-2 Spike RBD with a LOD of 4.86 ng mL^{-1} without using any labeling.

Nowadays, the most robust site-direct approach to date is based on the use of the biotin/avidin system in which antibodies are previously modified covalently with biotin to form a nearly irreversible interaction (exhibiting a K_D around 10^{-15} M), with streptavidin or avidin surfaces.[142,143,183,184] This immobilization route confers high efficiency on the sensor, and it is still used in bio-similarity assessment and drug discovery. This approach was explored in work by Nakhjavani et al.[185] who developed an electrochemiluminescent (ECL) sandwich immunosensor for the detection of carcinoembryonic antigen (CEA). The streptavidin/biotin binding was employed to bind the capture Ab to the AuNPs-modified GCE and to load the detection Ab and the HRP enzyme on luminol-modified AgNPs to perform the immunoassay. This approach showed improvement in the sensitivity of the layer-by-layer modified platform of Zang et al. from 0.3 pg/mL to 58 fg mL^{-1}. However, one of the limitations of this technique is given by the requirement of the previous step of chemical manipulation of the Ab, as well as the addition of one more protein (avidin/streptavidin) for each immobilization step, which contributes to improving cost of sensor realization.

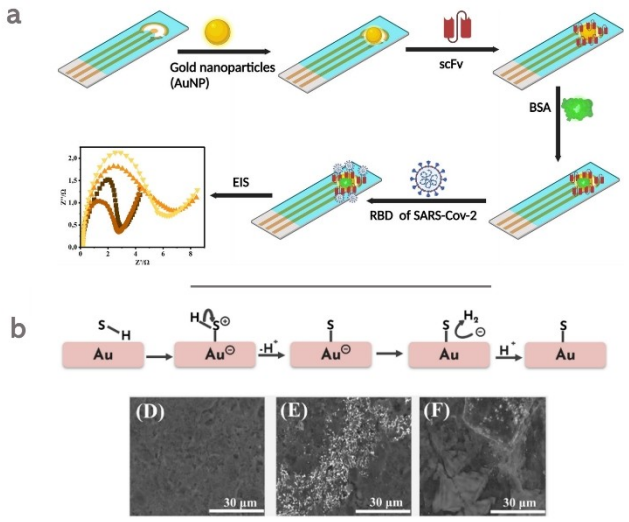

Figure 8. a) Stepwise modification in the assembly of the immunosensor developed by Fadhilah et al. b) Represent the scFv immobilization on AuNPs modified electrode in scheme and in SEM microscopy. Reprinted with permission from Ref. [182]. Copyright 2023, Wiley.

The use of biomolecules can be avoided by employing small molecules able to bind Fc region, N-glycosylation sites inside the Ab structure, or other artificial linkers. Among them, cyclic oligomers like calixarenes and resorc[4]arenes have been reported to entertain host-guest interaction with antibodies via their amino-residues, but with a different mechanism with respect to all other linkers.[186,187] As discussed earlier, the dipole moment of the whole IgG molecule is pointing from Fc to the $(Fab)_2$ fragment.[156,157,160,188] As a result, according to calixarenes dipole moment calculations, a minimum of energy occurs when this oligomer interacts with IgG in the *end-on* configuration,.[148,189,190] Their advantage is not limited to the Ab particular orientation, but they also allow anchoring biomolecules without requiring any activation step.[187,191] Their lower rims are often modified with thiols head groups to bind metal surfaces (i.e., gold, silver). In contrast, their upper rim is functionalized to ensure proper control over IgG orientation.[149] Although those structures have been primarily applied to modify solid supports,[148,149,192–195] those attracting features have made the calix[4]arene design suitable for NPs decoration. Recently, several works have been report using calix[4]arene modified NPs.[193,196–199] Among the electrochemical ones, Calcaterra et al.,[200] recently designed a resorc[4] arene-modified Au@MNPs for atrazine detection. The cyclic oligomer has been functionalized in the upper rim with carboxylic groups to improve its water solubility. In contrast, the lower rim has been modified with thioether headgroups able to interact with gold. The sensor performance of the resorc[4]arene -based Ab immobilization was then compared to those obtained by the classical EDC/NHS crosslinking, pointing out a sensitivity increasing from 18 to 46 μA mL ng^{-1} cm^{-2}.

Finally, one of the NPs-Ab immobilization methods that cannot be overlooked is the use of bacteria-derived proteins. Ab immobilization using Protein A or Protein G[187,201] is widely reported in the state-of-art as one of the most effective systems for Ab orientation.[202] These proteins originate from staphylococcal and streptococcal pathogenic strains and have structural domains that can recognize different IgG Fc fragments, thus letting the Fab region far from the electrode surface and, therefore, free to bind the analyte.[203]

The A or G protein-mediated strategy allows the Ab capture in an *end-on* orientation without any prior modification but keeps serious drawbacks such as the high costs. An interesting employment of the protein G-Ab binding was described by Khaniani et al.[204] in developing a portable SARS-CoV-2 serolog-

ical immunosensor. Herein, an Interdigitated Electrode (IDE) array was arranged to detect SARS-CoV-2 Antibodies in serum. The IDEs' surface was primarily functionalized with the Spike (S) protein to detect anti-SARS CoV-2 Ab eventually present in the real matrix. Protein G was loaded on AuNPs and was used to probe for bound antibodies exploiting their high affinity for Fc's IgG portion. The so-obtained immunosensor could discriminate between COVID-19 positive and negative sera. A less expensive immobilization technique to couple Fc region of Abs involves using boronic linkers for surface modification. Under their electron deficiency, Boronic acids possess an empty *p* orbital that can coordinate basic molecules and compounds with lone pairs like antibodies carbohydrate moieties placed in the Fc region.[142,151] The applicability of this strategy is not limited to antibodies but can be extended to all proteins in which carbohydrate moieties with 1,2-diols are placed far from the interaction site.[151,205] Heshemi et al. described an example: modified magnetic graphene nanoribbons (MGNRs) with boronic acid to immobilize anti-CD20 antibodies in the end-on orientation (Figure 9), increasing the sensor sensitivity.[206] The sensor was then incubated with blood samples to detect CD20 receptors of lymphoma cancer cells with highly sensitivity ranging around 38 cells/mL. This sensitivity is comparable with those of commercial flow cytometric assays.

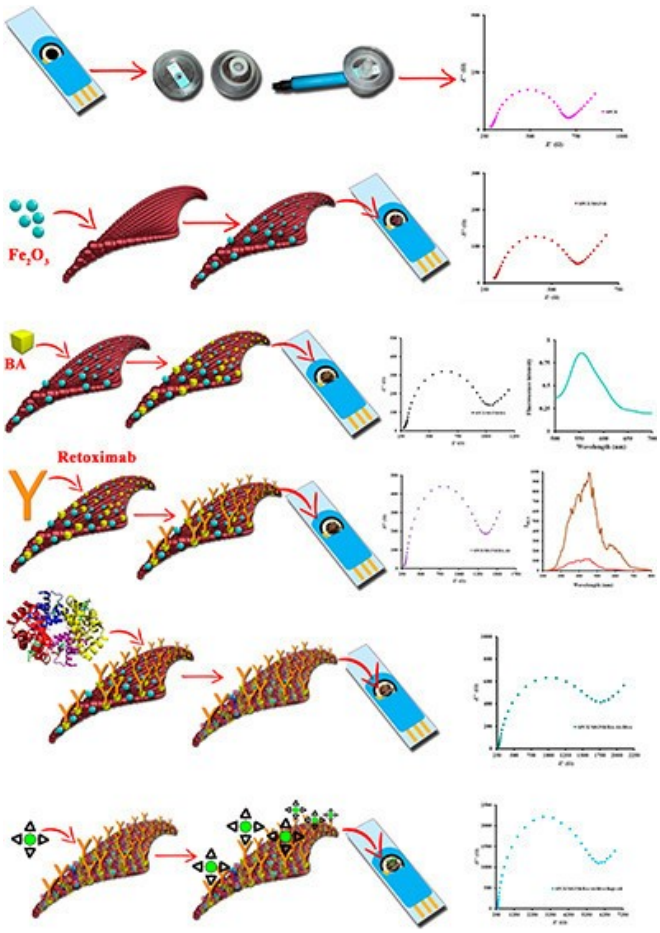

Figure 9. Scheme of fabrication of impedimetric immunosensor of Hashemi et al. with Rituximab Abs well-oriented by BA (boronic acid) pretreatment. Reprinted with permission from Ref. [206]. Copyright 2020, America Chemical Society.

4. Detection techniques

4.1. Voltammetric and amperometric immunosensors

Voltammetry and amperometry techniques are among the most used for realizing immunosensors due to their reproducibility, ease of use, and precision. Furthermore, the development of portable potentiostats and – more recently – smartphone interfaced has sparked significant interest in these procedures as improvements in the diagnoses on the field.[207,208] Voltammetric sensors, in brief, aim to measure changes in current occurring before and after the formation of the immune complex by scanning the potential in the interval near the reduction potential of an electroactive molecule, free in solution or bound to the surface. Depending on the applied potential, voltammetry is classified as LSV (Linear Sweep Voltammetry), DPV (Differential Pulse Voltammetry), SWV (Square Wave Voltammetry), and CV (Cyclic Voltammetry).[140,209] DPV is particularly useful in immunosensing due to its high efficacy in excluding capacitive current that typically arises during Ab adsorption. This consideration enables more precise monitoring of the faradic peak current variation due to antigen binding. Another technique that has been extensively utilized in immunosensor detection is chronoamperometry (CA). Conversely to what is described for DPV, this technique is performed by applying a potential step to the working electrode and measuring the current signal variation over time that usually follows the immunocomplex formation. Both DPV and CA can monitor the current variation of the redox probe anchored to the surface or free in solution. Recently, marked sandwich systems received great attention as the detection of Ab is covalently conjugated to a biological or non-biological element capable of catalyzing an electrochemical reaction of a redox mediator present in the solution. An example widely reported is based on the use of HRP-labeled detection antibodies capable of catalyzing the H_2O_2 reaction of its mediator dissolved in the electrochemical cell,[210,211] Figure 10. The antigen concentration increases as the amount of HRP on the sensor surface, causing an increase in the electrochemical signal produced, reported vs. the concentration.[131,212–214] However, several novel detection strategies have been recently reported to employ NPs in nanocomposites as mimicking-enzyme with catalytic activity for H_2O_2 reaction instead of HRP or other native enzymes.[215,216] To this aim, PdNPs have been recently used[217–219] as their particular efficiency in catalyzing the H_2O_2 reaction via a peroxide-oxide mechanism, thus enhancing electrochemical signal and sensors sensitivity, Figure 10b, c. Another set up suitable for DPV and chronoamperometry techniques follows the current variations due to a redox probe that is free in solution. Toluidine blue and ferricyanide are two mediators commonly used and reported on this platform. In such cases, unlike for what concerns the labeled immunoassays, the steric hindrance occurring after the antigen interaction

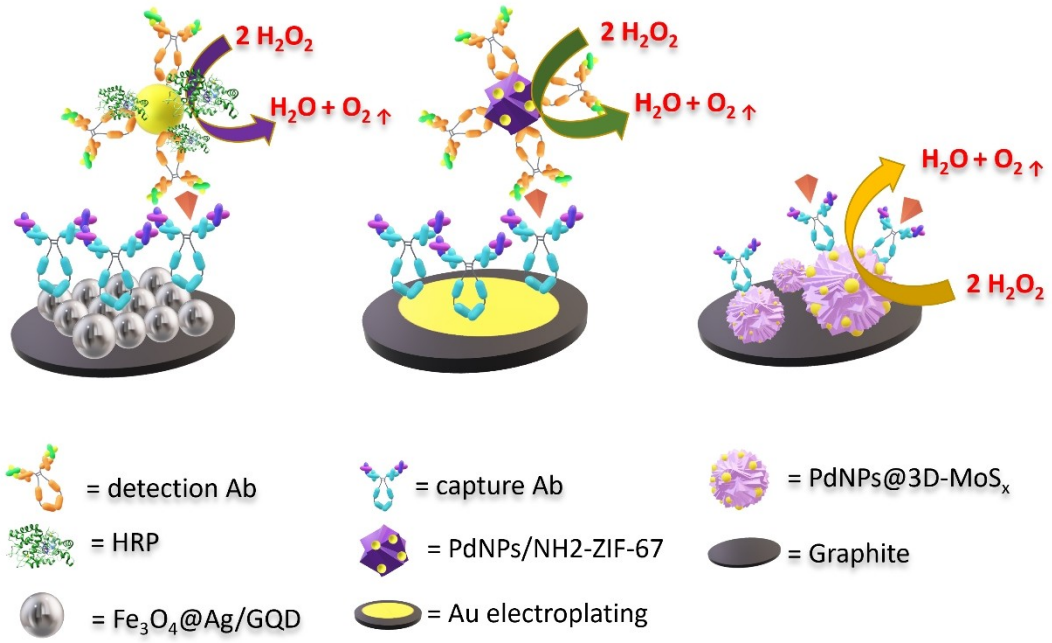

Figure 10. Most described approaches for NPs role in voltammetric and amperometric immunosensors a) including: signal amplifiers for HRP labeled antibodies and catalysts for b) PdNPs/NH2-ZIF67 described by Dai et al. Readapted with permission from Ref. [221]. Copyright 2019, Elsevier. c) PdNPs@3DMoSx (Gao et al.). Readapted with permission from Ref. [219]. Copyright 2019, Elsevier.

generally induces a decrease in redox probe peak current. Therefore, signal amplification is strongly required to achieve good sensitivity. To this aim, the surface of the sensing platform is often decorated with different NPs (i.e., AuNPs or Fe_3O_4 NPs). As reported by Huang et al.,[220] a high signal amplification can be obtained by adding AuNPs to a CNTs network's modified platform. The obtained Au@PEI@CNFs-based immunosensor was conductive enough to discriminate between the different concentrations of antigen (aflatoxin B1). The current decrease of ferrocyanide induced by the immunocomplex formation was then plotted vs. AFB1 achieving an excellent linear range between 0.05 to 25 ng mL^{-1}. On the other hand, several recent studies have been reported as detection strategies based on monitoring the oxidation or reduction of metals originating from the NPs to which the detection antibodies are loaded. Interestingly, in this setup, the NPs plays a dual role as protein carrier and electrochemical label.

The sensor surface of the sandwich immunosensor, reported by Tufa et al.,[127] is designed with detection antibodies anchored on AuNPs. As soon as they interact with the culture filtrate protein (CP-10) antigen, a potential of 1.3 V is applied to oxidate all the Au° bounded to the sensor surface. Subsequently, a reduction potential is used, and the electrochemical signal obtained by the gold reduction is plotted against the antigen concentration to build the calibration curve. This detection route has also been described for other metal NPs like copper[48,221] and silver.[222]

4.2. Nanoparticles as signal tags

Different routes of signal amplification can also be obtained by using NPs as signal tags to achieve wider linear range and enhanced performances. Many works have been reported over years in which enzyme-NPs bioconjugates has been employed to catalyse the deposition of other metals. To this aim, Guosong Lai et al.[222] developed a sandwich electrochemical immunosensor in which the Alkaline phosphatase (ALP) bind to Ab'/AuNPs conjugates, catalyses the formation of an indoxyl derivative that is able to reduce Ag+. The silver deposition, improved both by ALP and AuNPs presence, was then detected by anodic stripping voltammetry. This set up, allows to rich an incredibly wide linear range and leads to a LOD of 6.1 pg/mL. However, AgNPs can be also employed thanks to their ability to interact with streptavidin and thus to load biotinylated detection Abs on its surface (*as discussed in Section 3*). For instance,[223] silver NPs can be deposited in situ on CNT's and, after the biotinylated Ab' immobilization via streptavidin, the silver signal can be detected by ASV. This platform was also validated on serum samples, resulting in good accordance with the reference method. Another example of tracing tag for detection antibody was developed by Lin et al.[224] by exploiting the ability of AuNPs to catalyse the deposition of silver deposition. This electrochemical immunosensor, was designed by coupling the proteins with polystyrene-microacrilic acid beads (PSA) and AuNPs obtained by using $NaBH_4$ as reducing agent. Once the sensor was developed as depicted in Figure 11a, the silver stripping signal can take advantage of the synergic amplification led also by graphene immobilized on the electrode surface

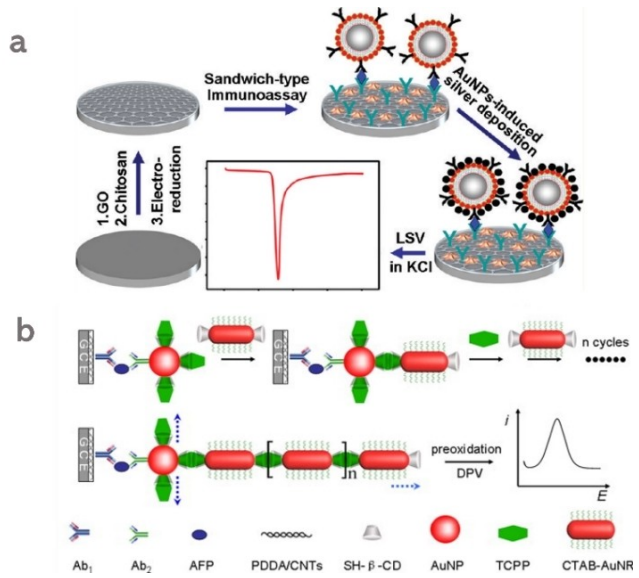

Figure 11. a) Scheme of sensor development described in the work of Lin et al. Readapted with permission from Ref. [224]. Copyright 2012, American Chemical Society. CD-AuNRs assembly presented by Lin et al. b) Readapted with permission from Ref. [225]. Copyright 2013, Elsevier.

and the poly(styrene-co-acrylic acid) leading to a LOD down to sub pg mL^{-1} level.

Gold nanostructures has been also variously employed as electroactive tracer. An interesting set up was presented from Dajie et al.[225] Herein, the signal antibody was loaded on AuNRs exhibiting thio-β-cyclodextrin (thio-β-CD) on the surface. Once the sandwich immunoassay was performed, the platform was further treated with 4,4,4,4-(21H, 23H-porphine-5,10,15,20-tetra-yl) tetrakis benzoic acid (TCPP), a molecule able to perform a host-guest interaction within two different cyclodextrin mojeties (Figure 11b). This phenomenon, leads CD-AuNRs to rapidly assembly on the immunosensor surface, improving the gold anodic signal recorded by DPV.

4.3. Impedimetric immunosensors

During the last decade, electrochemical impedance spectroscopy (EIS) has received wide attention as a detection technique in immunosensors, with the possibility of fingerprinting the electrode interfacial regions before and after biological interaction phenomena. By evaluating the variation in charge-transfer resistance (R_{ct}) or double layer capacity (C_{dl}) at the working electrode surface, the affinity of binding between the Ab and the Ag is easily detectable.[226] Moreover, this technique provides for two different types of measurement set-up: faradaic and non-faradaic EIS. The first requires a redox probe in solution and is largely employed in label-free electrochemical immunosensors development.[227] The second does not require any redox species or label. For this reason, the non-faradaic immunosensors are defined as redox-free and label-free platforms.[228] Applying alternating current to an electrochemical cell induces a specific response depending on the resistance produced by each element within the cell. Nyquist plots are generally used to analyze the response, where the imaginary part of impedance (Z_{Im}) is reported in the function of the real part (Z_{Re}), both collected under different frequencies (ν). The result is a curve that provides the Rct and Cdl values, which are specific for the analysed system from a proper fitting procedure.

The EIS-curve fitting can be made considering an equivalent circuit composed of each cell element contribute. The main circuit employed is called Randles circuit, consisting of the solution resistance (R_s) connected in series to double-layer capacitance (C_{dl}), charge-transfer resistance (R_{ct}) and diffusion resistance (Z_w), also called Warburg impedance. The R_{ct} and Z_w are considered only in the presence of a redox probe, thus in case of faradaic set ups.

Considering faradaic immunosensors, the interacting Ag is quantified through the R_{ct} variation. The increased steric hindrance onto the working electrode surface is responsible for a consequent increase in R_{ct}, due to more difficult diffusion of the redox probe through the biological non-conductive layer.

In this setup, if the electrode material is not improved in conductivity, the sensor's sensitivity results low. Core-shell Au@AgNPs have been employed to promote a decrease in R_{ct} working electrode and the bioreceptor optimal immobilization at the same time for the realization of a faradaic-impedimetric immunosensor detecting iron homeostasis biomarker hepcidin.[229] The same approach was adopted by using PdNPs-CNTs composites,[230] AuNPs@PEDOT[231] and AuNPs@MNPs[232] for detecting zearalenone (ZEN) in corn samples, SARS-CoV-2 antibodies in human serum and calreticulin (CRT) breast cancer biomarker respectively. Laser-induced one-step synthesis of Au, Ag, and PtNPs have been optimized by You and co-workers[233] and the three MeNPs were compared in impedimetric performance towards the redox couple $K_3Fe(CN)_6/K_4Fe(CN)_6$. AuNPs gave the lowest R_{ct} and have been employed to develop an impedimetric faradaic immunosensor for detecting *Escherichia coli* O157:H7. Another example of a label-free faradaic system was realized by modifying a glassy carbon electrode with Au nanorods (AuNRs) decorated graphitic carbon nitride (g-C_3N_4) (Figure 12a), immobilizing NS1 dengue biomarker Ab.[234] The composite promoted optimal ET, delivering a lower detection limit of 0.09 ng/mL. The combination of AuNPs with the 2D WS_2 nanoflakes in the realization of an immunosensor for human serum albumin (HSA) detection in human urine samples led to an EIS response three times higher than that obtained in the absence of the nanocomposites or compared to the performance provided by the two nanostructures separately.[236] Similarly, the coupling of AuNPs with graphene (GN) in a device for brain natriuretic peptide (BNP) quantification as a biomarker for several heart diseases decreased the starting R_{ct} of about eight times to the unmodified electrode.[237]

Unlike faradaic immunosensors, non-faradaic ones don't need high conductive transducers to improve the device's sensitivity. The C_{dl} variation is given by the change in dielectric and layer thickness properties and is expressed by Eq. (1):[238]

$$\frac{1}{C_t} = \frac{1}{C_i} + \frac{1}{C_a} \quad (1)$$

C_t is the total C, C_i is the starting value, C_a is the capacitance after Ag binding. If C_i is too low, the first term becomes dominant, limiting the device sensitivity.

For this reason, the employment of NPs sounds contradictory in this case, as one of the main characteristics of these NMs is their incredibly high conductivity. However, other important properties of NPs can still be crucial in this case, such as effective Ab immobilizers, being highly biocompatible, and promoting the loading of large amounts of bioreceptor. Therefore, although the representative works using NPs in such devices are much less numerous than faradaic-based ones, some examples deserve to be mentioned. AuNPs have been used exactly as electrode material[239] for assisting and improving the anti-D dimer (anti-DD) immobilization onto a carbon-based SPE to develop a non-faradaic impedimetric immunosensor detecting DD in blood samples. Similarly, carbon nano onions (CNOs) 5 nm size were used for the realization of a redox and label-free non-faradaic immunosensor detecting the pancreatic cancer biomarker CA19-9.[235] In this case, a home-made Ag screen printed interdigitated electrode was developed and modified with CNOs-GO nanocomposites (Figure 12b) for reaching a compromise in optimal C_i starting value and efficient Ab immobilization. The sensor delivered a LOD of 0.12 U/mL, which was two times lower than that obtained by using GO alone, also increasing the upper limit of the linearity range from 70 to 100 U/mL.

Finally, ZnO/CuO nanocomposites constituted by ZnONPs and CuONPs ranging between 200–300 nm have been employed for modifying a glass substrate and realize an electrode platform for the non-faradaic determination of caspase 9 in mammalian cell culture.[240] The nano-surface showed exceptional capability of capturing anti-caspase 9 even by drying technique, delivering a lower concentration limit of 0.07 U/mL in real samples.

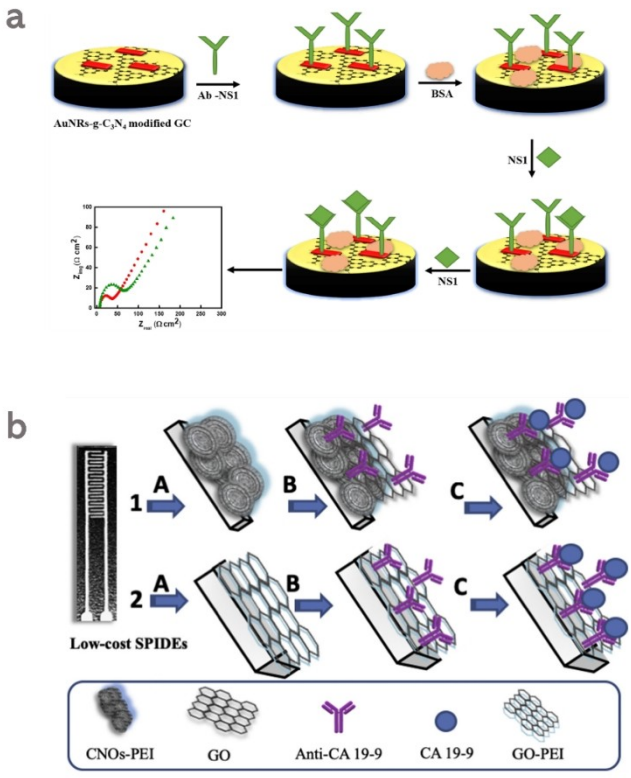

Figure 12. Scheme of fabrication of impedimetric immunosensors described in the work of : a) Ojha et al. Reprinted with permission from Ref. [234]. Copyright 2022, Elsevier. b) Redin et al. Reprinted with permission from Ref. [235]. Copyright 2019, Elsevier.

4.4. Field-transistor effect immunosensors

Ion-sensitive field effect transistors (ISFET) date back to 1970s, when Bergveld integrated for the first time a chemically sensitive layer with solid-state electronics.[241] Since then, FET-based immunosensors have dramatically attracted attention in the electronic smart-biosensing scenario. Briefly, ISFET is based on the measurement of the conductance between two electrodes (source, S and drain, D), modulated by a third element composed of an interface membrane/electrolyte solution capacitively coupled to an insulating material, Figure 13a.[242] When the membrane is non-polarizable, applying a certain potential VG (between such membrane and the semiconductor) exploits charge transfer (CT) with the solution analyte. The produced current is proportional to the analyte amount performing the CT. Conversely, when this principle is applied to immunosensors, the membrane is polarized and functionalized with Abs. Therefore, on the one hand, any CT phenomenon with the solution is avoided, and the eventual current produced is only due to the adsorption of charged molecules; on the other hand, the Ag, specific for the Ab bound to the membrane, can preferentially adsorb the interface. Being Abs, Ags and proteins charged molecules, this set-up can detect conductance variations due to increasing Ag amounts. These FET-based immunosensors, Figure 13b, are also called immunologically sensitive FET (IMFETs)[243] and are included in label-free and redox-free devices.

Their sensitivity is mainly affected by two factors: i) the thickness of the Debye layer forming at the membrane/solution interface when V_G is applied;[244] ii) the entity of the biological

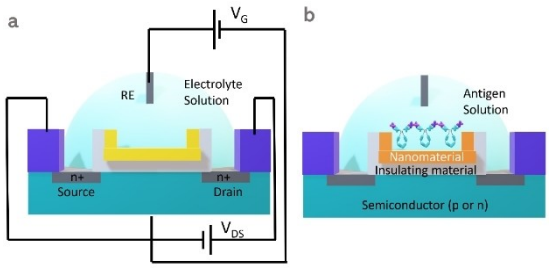

Figure 13. a) ISFET and b) IMFET set-up schemes. The ISFET set-up is converted into IMFET by immobilizing Ab molecules onto the gate.

recognition event depending on the limited number of the membrane surface binding sites for the Ab.[245] The first issue could be solved by diluting the electrolyte solution, allowing the increase in the Debye length and the incorporation of the Ag and part of the Ab inside the double layer. However, the conductance would strongly decrease, leading to the same initial problem. Therefore, Ab cleavage, bringing the Ag within the Debye length, is generally preferred.[181,246] The second issue is quickly addressed by employing nanostructures in sensor materials development.[247] NPs, in general, as a large surface-to-volume ratio, can offer numerous binding sites for biomolecules, allowing huge amounts of bioreceptor loading. Besides, they provide for enhancing in the overall gate conductivity. Although the focus for years was more placed on the optimization of 2D NMs in realizing IMFETs sensors, NPs such as CNTs, SiNWs, CDs, ZnONRs and calchogenide nanoribbons (NRBs) have also been investigated. ZnONRs have been used for modifying a SiO_2 transducer in a FET-immunosensor for human serum albumin (HSA), highly improving the availability of binding sites for the related Ab.[248] ZnONPs deliver high adsorption efficiency towards many biomolecules, as their isoelectric point (pI) of 9.5 promote strong attractive coulombic forces with lower pI bioreceptors.[249] The above-mentioned FET-immunosensor was able to detect HSA with a sensitivity of 0.826 mA/(g/mL), exhibiting a wide linear range between 0.01 and 100 mg/mL and LOD = 9.81 ng/mL. TiS_3 nanoribbons (TiS_3NRBs) of some nanometres thick and width lower than 500 nm also represented a good choice as a channel material in IMFET design for detecting CA 19–9 pancreatic cancer marker.[250] By synthesizing NRBs approaching the size-range of NPs, optimal S/D connection was achieved, as their superior packing ability, besides improving Ab linkage. Although, spherical and cylindrical surfaces proved to be much more efficient in enhancing the diffusion of the target toward the channel. The employment of CDs for planar graphene (GN) modification (Figure 14) has been a valid chance to realize an ultra-sensitive IMFET for detecting exosomes released by cancer cells.[251]

CDs acted as antennas, decreasing the LOD of GN-based IMFETs by three orders of magnitude without varying any GN structural property. In another work, SiNWs have been functionalized with SAM of silane-PEG-NH_2/silane-PEG-OH and conjugated to anti-Amyloid β (anti-Aβ), for determining the specific marker of Parkinson's disease Aβ 1–42 in human serum.[252] In this set-up, combining SAM-functionalized SiNWs with an aptamer as bio-amplifier was crucial for reaching a 100 fg/mL LOD, avoiding the very low Debye length typical of SiNWs-based IMFETs. CNTs also showed optimal performances in promoting the sensitivity and stability of such devices. Rabbani et al.[253] realized a CNT-based IMFET sensor for detecting C-reactive protein (CRP) in human serum as a biomarker for diagnosis of cardiovascular risk, type-2 diabetes, metabolic syndrome, hypertension, and various types of cancers. Specifically, CNTs have been deposited onto Si/SiO_2 support and functionalized with 1-pyrenebutanoic acid succinimidyl ester (PBASE) linker for binding anti-CRP. The system provided a wide linearity range between 0.01 and 1000 mg/mL, besides a LOD of 0.06 mg/mL. The stability evaluation after 120 days of storage showed a 94% signal retention.

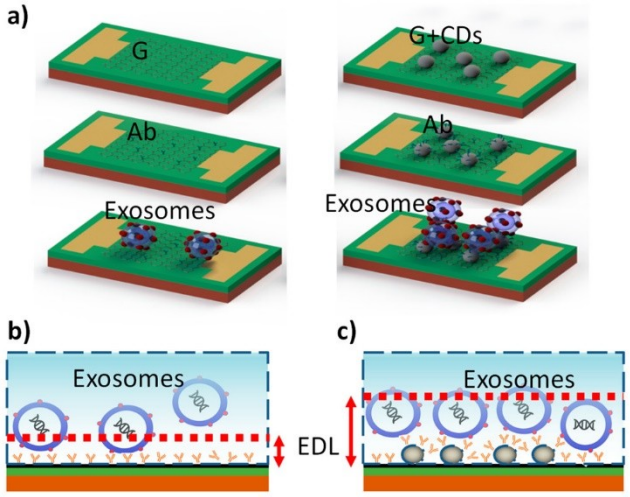

Figure 14. Scheme of assembly of the FET immunosensor, a) stepwise modification of the gate; b, c) electrochemical Debye length (EDL) variation in absence and presence of CDs respectively. The FET immunosensor is described in the work of Ramadan et al. Reprinted with permission from Ref. [251]. Copyright 2021, American Chemical Society.

5. Perspective and future trends

In recent years, medical diagnostics and chemical analysis in the fields of the environment and food are being revolutionized by the emerging technologies of electrochemical immunosensors. These sensors can quickly and accurately identify biomarkers in the examined sample by intelligently and selectively detecting their presence. One of the significant advances in this field is paper-based immunosensors. They have good properties, such as flexibility, lightness, hydrophilic, fibrous, and porous structure, making them easy to use and convenient. These devices use paper substrates with specific antibodies to identify a biomarker of interest. They can be functionalized with nanomaterial like MWCNT for detecting the avian influenza virus[254] and AuNPs for detecting cytokines to determine the health status of COVID-19 patients.[255] Paper-based immunosensors have several benefits, such as low cost, simplicity of use, and potential for downsizing, making them suited for field usage and resource-constrained scenarios. Another widely used type of electrochemical immunosensor is lateral-flow immunosensors. These devices generally consist of a nitrocellulose strip functionalized with antibodies for recognizing specific antigens, conjugate pads, sample pads, and absorbent pads that have been appropriately bonded together and put on a support card. A sample pad injects the sample solution, which is transported to other components by capillary force. The conjugate pad offers a layer pre-deposited by a bioreceptor target that has been marked and binds to the target biomolecules.The control and capture targets, which serve as the control and test lines, are pre-anchored using the NC

Table 1. Most relevant NPs-based electrochemical immunosensors published in the literature during the last six years.

NPs	Role	Electrochemical platform	Label(s)	Immunosensor type	Target	Detection	Application field	Ref.
Flower-like AgNPs	Signal Amplifier	Flower-like AgNPs/ MoS_2/rGO/GCE	–	I-f	CEA	CA	*Diagnostic*	[273]
AuNPs	Signal Amplifier	AuNPs/CNOs/SWCNTs/ CS-NC/GCE	–	I-f	CEA	SWV	*Diagnostic*	[274]
CS-AuNPs	Nanocarrier	Ab1-CS-AuNPs/ MWCNTs/GO/GCE	AuNPs-Ab_2-LOx	s-w	CA125	CA	*Diagnostic*	[82]
AuPdCu/ N-GQDs@PS	Signal Amplifier/ Antibody Loading	BSA/Ab/AuPdCu/ N-GQDs@PS/GCE	–	I-f	HBsAg	CA	*Diagnostic*	[275]
Pd@Au@Pt Nano-strucrures	Signal Amplifier/ Antibody Loading	Ab-Pd@Au@Pt NPs/ COOH-rGO/AuSPE	–	I-f	CEA and PSA	DPV	*Diagnostic*	[276]
Au@Ag-Cu_2O NPs and Au@N-GQDs	Signal Amplifier/ Antibody Loading and Nanocarrier	Ab1-Au@N-GQDs/ GCE	Ab_2-Au@Ag-Cu2O	s-w	PSA	CA	*Diagnostic*	[277]
Ag/MoS2@Fe3O4 and AgNPs	Nanocarrier and Signal Amplifier	Ab1-AgNPs/MGCE	Ab_2-Ag/ MoS2@Fe3O4-modiefied MGCE	s-w	CEA	DPV	*Diagnostic*	[278]
AuNPs and (AuPt-MB) nanorods	Antibody Loading and Nanocarrier/ Ectroactive tracer	Ab1-AuNPs@N-GNRs-Fe-MOFs/GCE	Ab_2-AuPt-MB	s-w	Galectin-3	DPV	*Diagnostic*	[279]
SiO_2NPs	Antibody Loading	Ab-SiO_2NPs/poly electrolytes multilayer (PEM)/AuSPE	–	I-f	Escherichia coli	CV	*Diagnostic*	[280]
AuPtNPs	Antibody Loading	MO/CNT-Au/ Ab_2 label	Ab_1-AuPt-vertical graphene/glassy carbon electrode	I-f/s-w	alpha-fetoprotein	DPV	*Diagnostic*	[281]
Au@MoS2/C S nanocomposite	Signal Amplifier/ Antibody Loading	Ab-Au@MoS 2/ Chitosan-modified GCE	–	I-f	MSG	DPV	*Food*	[282]
PtCoCuPd alloyed tripods	Signal Amplifier/ Antibody Loading	BSA/Ab-PtCoCuPd HBTPs/GCE	–	I-f	cTnI	DPV	*Diagnostic*	[283]
Au@MNPs	Signal Amplifier/ Antibody Loading	Ab_1/RW/Au@MNPs/ SPCE	–	I-f	ATZ	DPV	*Environmental*	[200]
AuNpS	Signal Amplifier/ Antibody Loading	Ab-Au nanoparticles/ Zn/Ni-ZIF-8-800@graphene	–	I-f	Monensin in milk	CV	*Food*	[284]
MXene@AuNPs	Signal Amplifier	Ab1-AuNPs-ATPGO/ GCE	Ab_2-d-$Ti_3C_2T_x$ MXene@AuNPs	s-w	PSA	DPV	*Diagnostic*	[285]
PtNPs-rGO-PSNS	Antibody loading/ Signal amplifier	Ab-PtNPs@rGO @PS NS/GCE	–	I-f	CEA	DPV	*Diagnostic*	[286]
AuNPs	Signal Amplifier/ Antibody Loading	Ab-AuNPs/FTO	–	I-f	SARS-CoV-2 Spike S1 antigen	DPV/CV	*Diagnostic*	[287]
nLa_2O_3NPs	Antibody loading/ Signal amplifier	BSA/ab-APTES/ nLa2O3/ITO	–	I-f	CPX	DPV	*Food*	[288]
Popcorn-shaped PtCoCuNPs	Signal Amplifier	Ab-PtCoCu PNPs/ NB-rGO/GCE	–	I-f	β-Amyloid1-42	CA	*Diagnostic*	[289]
MNPs	Antibody Loading	Ab-MNPs@protG/ PB/H-PAu-AuSPE	–	I-f	ATZ	DPV	*Environmental*	[290]
TiO2 NPs	Signal Amplifier/ Antibody Loading	BSA/Antigen/ TiO2-CS/GCE	–	I-f	SARS-CoV-2 antibody	DPV	*Diagnostic*	[291]
Gd_2O_3 NPs	Antibody Loading	BSA/anti-CT/ APTES-Gd2O3/ITO	–	I-f	CT	CV	*Diagnostic*	[292]
AuNPs	Nanocarrier	A disposable micro-fluidic device (DμFD) comprising an array of SPE	Ab_2-AuNPs	s-w	Salmonella typhimurium	DPV	*Food*	[293]
AgNPs	Electroactive tracer	GCCE	Ab_2@AgNP	s-w	Tick-Borne Encephalitis	LSV	*Diagnostic*	[294]
Au NPs and AgNPs @microporous carbon spheres	Signal Amplifier/ Antibody Loading	Au NPs/GCE	Ag NPs@-MCS Hemin/rGO-Ab_2	s-w	CEA	CA	*Diagnostic*	[295]
MoS_2@Cu_2O-Pt Nanohybrid	Nanocarrier	Ag/BSA/Ab_1/PGO/ Au/GCE	MoS_2@Cu_2O-Pt-Ab_2	s-w	Hepatitis B Surface Antigen	CA	*Diagnostic*	[99]
AuNPs and PdNPs	Antibody Loading and Nanocarrier	BSA/Ab_1-Au/GCE	Ab_2-Pd/NH2-ZIF-67 marker	s-w	prostate-specific antigen	CA	*Diagnostic*	[221]
AuNPs and Au@Ag NPs	Antibody Loading and Nanocarrier	Ab_1/D-Au NPs/GCE	Au@Ag/PDA-PR-MCS-Ab_2	s-w	α-fetoprotein	CA	*Diagnostic*	[296]
AuNPs and Au@PtDNs	Signal Amplifier and EC tracer	Ab_1-PDA@Au NPs/ GCE	Au@Pt DNs/ NG/$Cu2^+$-Ab_2	s-w	CEA	CA	*Diagnostic*	[297]
AuNPs and Au@Pd NDs	Antibody Loading and EC tracer	Ab_1-GS-NH_2/AuNPs/ GCE	Au@Pd NDs/ Fe2+-CS/ PPy NTs-ab_2	s-w	CEA	CA	*Diagnostic*	[298]

Table 1. continued

NPs	Role	Electrochemical platform	Label(s)	Immunosensor type	Target	Detection	Application field	Ref.
Trimetallic PdPtCu NPs	Nanocarrier	GCE/Au NPs/Ab_1/BSA/PSA	Ab_2-PdPtCu	s-w	PSA	DPV	*Diagnostic*	[299]
IrO_2 NPs	EC tracer	MBs-PBDE-IrO_2NPs/SPCE	–	l-f	PBDEs	CHA	*Environmental*	[300]
Au@MNPs	Antibody Loading	Ab_1/Cys/Au@MNPs/SPCE	–	l-f	25-OHD3	DPV	*Diagnostic*	[138]
Pd NPs@3D MoSx	EC tracer	Pd NPs@3D MoSx/GCE	–	l-f	insulin	CA	*Diagnostic*	[46]
GQDs@ZrO2	EC tracer	BSA/ab-GQDs@ZrO2/ITO	–	l-f	OTA	DPV	*Food*	[55]
Octaedral AuNPs	Nanocarrier/ Signal Amplifier	Ab_1-Au oct/GCE	Au oct PCs-TB@Ab_2	s-w	OTA	SWV	*Food*	[301]
$Ni(OH)_2$NPs	Antigen Loading	Ag- $Ni(OH)_2$ NPs/SPCE	–	l-f	SARS-CoV-2	DPV	*Diagnostic*	[302]
AgNPs@SWCNHs	Nanocarrier	Ab_1/Ag/BSA/Au NDs/GCE	Ab_2@Ag NPs @SWCNHs	s-w	sulphonamides	LSV	*Environmental*	[54]
MWCNT-PDMS	Antibody Loading	Ab-MWCNT-PDMS/paper-based sensor	–	l-f	Avian influenza virus antigens	DPV	*Diagnostic*	[254]
Ag@AuNPs	Antibody loading/ electrode material	Ab/Cys/Ag@AuNPs/FTO	–	l-f	HEP	EIS-F	*Diagnostic*	[229]
PdNPs-CNTs	Antibody loading/ electrode material	Ab/EDC-NHS/PdNPs-CNTs-CS/SPCE		l-f	ZEN	EIS-F	*Food*	[230]
AuNPs@MNPs	Antibody loading/ electrode material	Ab/EDC-NHS/AuNPs@MNPs/ITO	–	l-f	CRT	EIS-F	*Diagnostic*	[232]
AuNRs-g-C_3N_4	Antibody loading/ electrode material	Ab/AuNRs- g-C_3N_4/GCE	–	l-f	NS1	EIS-F	*Diagnostic*	[234]
AuNPs-PEDOT	Antigen loading/ electrode material	Ag/AuNPs-PEDOT/SME	–	l-f	SARS-CoV-2 antibodies	EIS-F	*Diagnostic*	[231]
ZnONPs-CuONPs	Antibody loading/ electrode material	Ab/ZnONPs-CuONPs/glass	–	l-f	Caspase-9	EIS-NF	*Diagnostic*	[240]
AuNPs-DHP	Antibody loading/ electrode material	Ab/AuNPs-DHP/SPCE	–	l-f	DD	EIS-NF	*Diagnostic*	[239]
CNOs-GO films	Antibody loading/ electrode material	Ab/CNOs-GOfilm/SPIDE	–	l-f	CA 19-9	EIS-NF	*Diagnostic*	[235]
SiNWs-APTES	Antibody loading/ gate material	Ab/GA/APTES-SiNWs	–	l-f	Aβ 1-42	FET	*Diagnostic*	[252]
ZnONRs-APTES	Antibody loading/ gate material	Ab/APTES-ZnONRs	–	l-f	HSA	FET	*Diagnostic*	[248]
CDs-2D-GN	Antibody loading/ gate material	Ab/CDs-2D-GN	–	l-f	exosomes	FET	*Diagnostic*	[251]
TiS_3NRBs	Antibody loading/ gate material	Ab/TiS_3NRBs/Au@SiO_2/Si	–	l-f	CA 19-9	FET	*Diagnostic*	[250]
CNTs	Antibody loading/ gate material	Ab/CNTs/SiO_2/Si	–	l-f	CRP	FET	*Diagnostic*	[253]

*NPs nanoparticles; Ab antibody; NCs nanocomposites; Ag antigen; l-f Label-free; s-w sandwich; DPV Differential Pulse Voltammetry; CV Cyclic Voltammetry; EIS-F faradaic electrochemical impedance spectroscopy; EIS-NF non-faradaic electrochemical impedance spectroscopy; FET field-effect transistor; LSV Linear Sweep Voltammetry; CHA chronoamperometry; SPCE Screen-Printed Carbon Electrode; GCE glassy carbon electrode; GCCE Gold-carbon composite electrode; MGCE magnetic glassy carbon electrode; FTO fluorine doped tin oxide electrodes; PDMS polydimethylsiloxane; MoS2 Molybdenumdisulfide; rGO reduced graphene oxide; SWCNTs single-walled carbon nanotubes; CNOs carbon nano-onions; CS Chitosan; GO graphene oxide; CEA carcinoembryonic antigen; HbsAg Hepatitis B surface antigen; BSA bovine serum albumin; PSA prostate specific antigen; GNR graphene nanoribbons; cTnI cardiac troponin I; PAMAM Polyamidoamine; RW resorc[4]arene, TB Tolouidine Blue; ATP p-aminothiophenol; PSNS polystyrene nanospheres; CPX ciprofloxacin; ATZ atrazine; PB Prussian Blue; MNPs magnetic nanoparticles; CT Vibrio cholera; NH2-ZIF-67 amino-zeolitic imidazolate framework-67; PDA polydopamine; PR phenolic resin; MCS microporous carbon spheres; DNs dendritic nanomaterials; PBDEs Polybrominated diphenyl ethers; OTA ochratoxin A; CNHs carbon nanohorns; PDMS polydimethylsiloxane; SWCNHs Single-Wall Carbon Nanohorns; AuNDs Gold nanodendrimers; Cys Cysteamine; HEP hepsidin homeostasis biomarker; ZEN zearalenone; CRT calreticulin; PEDOT Poly (3,4-ethylenedioxythiophene); SME steel mash electrode; DHP dihexadecylphosphate;DD D-dimer; CNOs carbon nano onions; SPIDE screen-printed interdigitated electrode; CA 19-9 cabohydrate antigen 19-9; SiNWs silicon nanowires; APTES (3-Aminopropyl)triethoxysilane; Aβ 1-42 amyloid beta 1-42; GA glutaraldehyde; HSA human serum albumin; ZnONRs zinc oxide nanorods; GN graphene; CDs carbon dots; TiS_3NRBs TiS_3 nanoribbons; CRP C-reactive protein.

membrane pad. The absorbent pad also develops capillary power, preventing the injected material from flowing backward and providing fast results, making them popular in diagnosing infectious diseases or determining herbicides such as atrazine and acetochlor.[256] After the COVID-19 pandemic, they were widely used for quick pathogen identification. Actually, electrochemical immunosensors have been replaced mainly by colorimetric ones.[257–259] Immunosensors created using 3D printers (or "3D-printed immunosensors") are an emerging trend in the electrochemical immunosensor industry. With the aid of this technique, very precise and unique sensors may be created utilizing biocompatible materials. The adaptability of 3D printing enables the creation of devices with various geometries and morphologies, improving detection efficiency.

3D-printed immunosensors have a lot of potential for use in personalized medicine since they may be customized, in shape and dimension, to meet specific diagnostic requirements. Often, the use of 3D printing technology has been applied to the creation of devices that can assist in detecting viruses, such as SARS-CoV-2[260] or chiral recognition.[261] A very last frontier of 3D printing technology is bioprinting, which allows producing organs and tissues through appropriate materials, such as intestinal microvilli used to modify electrochemical sensors to detect gliadin.[262] Finally, wearable immunosensors may be incorporated into clothes, medical equipment, or personal items. These sensors can identify biomarkers on the skin, providing real-time user health monitoring. Numerous benefits are provided by wearable immunosensors, including continuous monitoring, ease, and the capacity to send data to other devices for processing instantly. Due to their reduced invasiveness compared to more conventional techniques, including blood collection, they are frequently used to diagnose biofluids. Specifically, immunosensors for detecting cortisol present in sweat have been developed.[263,264] POCT immunosensors attracted great attention, thanks to their ability to achieve a rapid screening close to the site of patient care.[140,209] During pandemic, the need to improve the population screening has lead to immunosensing integration with recent advancements in digital technology.[265] In particular, the diffusion of Internet of Medical Things (IoMT)[266,267] aims to provide a network of Internet-connected medical devices while AI enables a quick and adaptable medical data analysis.[267,268] The work of Fortunati et al.[269] provided an example, combining machine learning for data processing and analysis with Spike S1 detection and the possibility to integrate the portable platform with a cloud-based portable Wi-Fi device. In this context, the use of AI can also facilitate the immunosensor[268] integration with other devices, such as smartphones and wearable sensors by using communication protocols and also enabling the ability to perform multiple functions simultaneously, such as diagnosis, prognosis or therapy monitoring.[267] Additionally, by enabling electrochemical signal decoupling[270] and multiple parameters analysis, machine learning can also be extremely important in the data analysis of electrochemical sensors, enhancing sensors accuracy and reliability.[269–272] In order to achieve this, Xu et al.[272] created an AI-powered EIS immunosensor for the detection of E. coli. In this work, bacterial concentrations were correlated not only with charge transfer resistance, as is commonly reported, but also with capacitance, resulting in a sensor with higher accuracy.

6. Summary and Outlook

An outlook on developing NP-based electrochemical immunosensors has been reviewed, focusing on the NPs role in protein conjugation, signal amplification, and detection. Different morphologies and synthetic roots pointing out their reactivity and applicability, were explored. Special attention was given to how their charges and nature can affect Ab interaction in terms of orientation and density. Ab-NPs conjugation techniques was reported focusing on how different immobilization routes can be applied to reach different nanostructures. Furthermore, their role in other electrochemical detection techniques was investigated. Last trends in amperometric and voltammetric immunosensors were explored, pointing out the critical role of NPs in developing new strategies for immunosensor detection, as the enzyme mimetic properties of novel NPs nanocomposite and the direct redox signal obtainment from the reduction of MeNPs. In EIS and FET, a crucial role of NPs is played in sensitivity enhancement. Concerning solid support modification, their gaining in conductivity allows them to explore different immunoassay setup and recognition strategies. In such cases, the challenge could be to tune the NPs features to improve the surface-to-volume ratio and the protein loading. In Table 1 are summarized the most cited and representative works published during the last six years, highlighting the NPs specific role, the immunosensor type, the detection technique employed, and the target and application field. Latest emerging technologies spreading in electrochemical immunosensing and their revolutionary potential in the diagnostic, food and environmental field, with a particular focus on paper-based hybrid electrochemical immunosensors, 3-D printing technologies and the integration of IoMT, POCT, AI in electrochemical immunosensors was also discussed.

Conflict of Interests

The authors declare no conflict of interest.

Data Availability Statement

Data sharing is not applicable to this article as no new data were created or analyzed in this study.

Keywords: nanoparticle-based immunosensors · bioelectrochemistry · affinity biosensors · nanotechnology · electrochemical immunosensors

[1] A. V. Police Patil, Y.-S. Chuang, C. Li, C.-C. Wu, *Biosensors* **2023**, *13*, 125.
[2] A. Iglesias-Mayor, O. Amor-Gutiérrez, A. Costa-García, A. de la Escosura-Muñiz, *Sensors* **2019**, *19*, 5137.
[3] M. Zahran, Z. Khalifa, M. A.-H. Zahran, M. A. Azzem, *Mater Adv* **2021**, *2*, 7350–7365.
[4] Y. Xiao, H.-X. Ju, H.-Y. Chen, *Anal. Chim. Acta* **1999**, *391*, 73–82.
[5] W. Zhang, R. Wang, F. Luo, P. Wang, Z. Lin, *Chin. Chem. Lett.* **2020**, *31*, 589–600.
[6] Z. Zhang, Y. Cong, Y. Huang, X. Du, *Micromachines (Basel)* **2019**, *10*, 397.
[7] E. B. Aydin, M. Aydin, M. K. Sezgintürk, *Adv. Clin. Chem.* **2019**, *92*, 1–57.
[8] C. Kokkinos, A. Economou, M. I. Prodromidis, *TrAC Trends Anal. Chem.* **2016**, *79*, 88–105.
[9] A. K. Trilling, J. Beekwilder, H. Zuilhof, *Analyst* **2013**, *138*, 1619–1627.
[10] J. Kim, M. Park, *Biosensors (Basel)* **2021**, *11*, 360.
[11] H. Filik, A. A. Avan, *Talanta* **2019**, *205*, 120153.
[12] P. B. Santhosh, J. Genova, H. Chamati, *Chemistry (Easton)* **2022**, *4*, 345–369.
[13] M. Mohammadlou, H. Maghsoudi, H. Jafarizadeh-Malmiri, *Int. Food Res. J.* **2016**, *23*, 446.
[14] R. Abou Gabal, D. Shokeir, A. Orabi, *Trends in Sciences* **2022**, *19*, 2062.

[15] I. Hussain, N. B. Singh, A. Singh, H. Singh, S. C. Singh, *Biotechnol. Lett.* **2016**, *38*, 545–560.
[16] A. Pollap, J. Kochana, *Biosensors (Basel)* **2019**, *9*, 61.
[17] R. Sharma, K. V. Ragavan, M. S. Thakur, K. Raghavarao, *Biosens. Bioelectron.* **2015**, *74*, 612–627.
[18] Y. Yang, G. Li, D. Wu, J. Liu, X. Li, P. Luo, N. Hu, H. Wang, Y. Wu, *Trends Food Sci. Technol.* **2020**, *96*, 233–252.
[19] X. Qi, Z. Wang, R. Lu, J. Liu, Y. Li, Y. Chen, *Food Chem.* **2021**, *338*, 127837.
[20] B. Nguyen, D. Claveau-Mallet, L. M. Hernandez, E. G. Xu, J. M. Farner, N. Tufenkji, *Acc. Chem. Res.* **2019**, *52*, 858–866.
[21] H. Nosrati, M. Salehiabar, M. Fridoni, M. A. Abdollahifar, H. Kheiri Manjili, S. Davaran, H. Danafar, *Sci. Rep.* **2019**, *9*, 10.1038/s41598-019-43650-4.
[22] M. Imran, A. M. Affandi, M. M. Alam, A. Khan, A. I. Khan, *Nanotechnology* **2021**, *32*, 10.1088/1361-6528/ac137a.
[23] S. Ahmed, A. Ansari, M. A. Siddiqui, M. Imran, B. Kumari, A. Khan, P. Ranjan, *Adv. Nat. Sci. Nanosci. Nanotechnol.* **2023**, *14*, 10.1088/2043-6262/aceda9.
[24] M. Vert, Y. Doi, K.-H. Hellwich, M. Hess, P. Hodge, P. Kubisa, M. Rinaudo, F. Schué, *Pure Appl. Chem.* **2012**, *84*, 377–410.
[25] R. Zumpano, F. Polli, C. D'Agostino, R. Antiochia, G. Favero, F. Mazzei, *Electrochemistry* **2021**, *2*, 10–28.
[26] R. Zumpano, F. Polli, C. D'Agostino, R. Antiochia, G. Favero, F. Mazzei, *Electrochemistry* **2021**, *2*, 10–28.
[27] H. Ju, *Appl. Mater. Today* **2018**, *10*, 51–71.
[28] S. Tajik, H. Beitollahi, M. Torkzadeh-Mahani, *J. Nanostructure Chem.* **2022**, *12*, 10.1007/s40097-022-00496-z.
[29] L. Suresh, P. K. Brahman, K. R. Reddy, J. S. Bondili, *Enzyme Microb. Technol.* **2018**, *112*, 10.1016/j.enzmictec.2017.10.009.
[30] B. D. Mansuriya, Z. Altintas, *Nanomaterials* **2021**, *11*, 10.3390/nano11030578.
[31] C. J. Edgcombe, U. Valdre, *J. Microsc.* **2001**, *203*, 188–194.
[32] P.-L. Hsieh, M. Madasu, C.-H. Hsiao, Y.-W. Peng, L.-J. Chen, M. H. Huang, *J. Phys. Chem. C* **2021**, *125*, 10051–10056.
[33] X.-L. Liu, J.-H. Wang, S. Liang, D.-J. Yang, F. Nan, S.-J. Ding, L. Zhou, Z.-H. Hao, Q.-Q. Wang, *J. Phys. Chem. C* **2014**, *118*, 9659–9664.
[34] X. Zhang, J. Qi, Q. Zhang, Y. Xue, F. Meng, J. Zhang, Y. Liu, G. Yang, C. Wu, *Microchim. Acta* **2023**, *190*, 10.1007/s00604-022-05618-6.
[35] Q. Wei, C. Wang, P. Li, T. Wu, N. Yang, X. Wang, Y. Wang, C. Li, *Small* **2019**, *15*, 10.1002/smll.201902086.
[36] L. H. Stanker, R. M. Hnasko, *Methods Mol. Biol.* **2015**, *1318*, 69–78.
[37] J. Lei, H. Ju, *Chem. Soc. Rev.* **2012**, *41*, 2122–2134.
[38] H. Ju, *J. Anal. Test* **2017**, *1*, 1–18.
[39] Z. Dai, F. Yan, J. Chen, H. Ju, *Anal. Chem.* **2003**, *75*, 5429–5434.
[40] J. Chen, F. Yan, Z. Dai, H. Ju, *Biosens. Bioelectron.* **2005**, *21*, 330–336.
[41] X. Yi, J. Huang-Xian, C. Hong-Yuan, *Anal. Biochem.* **2000**, *278*, 22–28.
[42] E. Ma, P. Wang, Q. Yang, H. Yu, F. Pei, Y. Li, Q. Liu, Y. Dong, *Biosens. Bioelectron.* **2019**, *142*, 10.1016/j.bios.2019.111580.
[43] T. Zhang, B. Xing, Q. Han, Y. Lei, D. Wu, X. Ren, Q. Wei, *Anal. Chim. Acta* **2018**, *1032*, 114–121.
[44] M. Awan, S. Rauf, A. Abbas, M. H. Nawaz, C. Yang, S. A. Shahid, N. Amin, A. Hayat, *J. Mol. Liq.* **2020**, *317*, 10.1016/j.molliq.2020.114014.
[45] Y. Liu, H. Wang, C. Xiong, Y. Yuan, Y. Chai, R. Yuan, *Biosens. Bioelectron.* **2016**, *81*, 334–340.
[46] Z. Gao, Y. Li, C. Zhang, S. Zhang, F. Li, P. Wang, H. Wang, Q. Wei, *Biosens. Bioelectron.* **2019**, *126*, 10.1016/j.bios.2018.10.017.
[47] L. Suresh, J. S. Bondili, P. K. Brahman, *Mater. Today Chem.* **2020**, *16*, 10.1016/j.mtchem.2020.100257.
[48] E. V. Dorozhko, A. S. Gashevskay, E. I. Korotkova, J. Barek, V. Vyskocil, S. A. Eremin, E. V. Galunin, M. Saqib, *Talanta* **2021**, *228*, 122174.
[49] L. Suresh, J. S. Bondili, P. K. Brahman, *Mater. Today Chem.* **2020**, *16*, 100257.
[50] M. S. Khan, W. Zhu, A. Ali, S. M. Ahmad, X. Li, L. Yang, Y. Wang, H. Wang, Q. Wei, *Anal. Biochem.* **2019**, *566*, 10.1016/j.ab.2018.11.010.
[51] Q. Lan, C. Ren, A. Lambert, G. Zhang, J. Li, Q. Cheng, X. Hu, Z. Yang, *ACS Sustainable Chem. Eng.* **2020**, *8*, 10.1021/acssuschemeng.9b06858.
[52] X. Lv, M. Bi, X. Xu, Y. Li, C. Geng, B. Cui, Y. Fang, *Anal. Bioanal. Chem.* **2022**, *414*, 1389–1402.
[53] J. Ran, D. Luo, B. Liu, *J. Solid State Electrochem.* **2023**, *27*, 399–408.
[54] Z. Zhang, M. Yang, X. Wu, S. Dong, N. Zhu, E. Gyimah, K. Wang, Y. Li, *Chemosphere* **2019**, *225*, 10.1016/j.chemosphere.2019.03.033.
[55] P. K. Gupta, D. Chauhan, Z. H. Khan, P. R. Solanki, *ACS Appl. Nano Mater.* **2020**, *3*, 10.1021/acsanm.9b02598.
[56] P. Assari, A. A. Rafati, A. Feizollahi, R. A. Joghani, *Mater. Sci. Eng. C* **2020**, *115*, 111066.
[57] Y. Feng, N. Wang, H. Ju, *Sci. China Chem.* **2022**, *65*, 2417–2436.
[58] C. Wang, S. Liu, H. Ju, *Bioelectrochemistry* **2023**, *149*, 10.1016/j.bioelechem.2022.108281.
[59] L. Yu, M. Li, Q. Kang, L. Fu, G. Zou, D. Shen, *Biosens. Bioelectron.* **2021**, *176*, 10.1016/j.bios.2020.112934.
[60] M. A. Sadique, S. Yadav, V. Khare, R. Khan, G. K. Tripathi, P. S. Khare, *Diagnostik* **2022**, *12*, 2612.
[61] Y. W. Hartati, L. K. Letelay, S. Gaffar, S. Wyantuti, H. H. Bahti, *Sens. Biosensing. Res.* **2020**, *27*, 100316.
[62] X. Yu, Y. Li, Y. Li, S. Liu, Z. Wu, H. Dong, Z. Xu, X. Li, Q. Liu, *Talanta* **2022**, *236*, 122865.
[63] E. M. Materón, C. M. Miyazaki, O. Carr, N. Joshi, P. H. S. Picciani, C. J. Dalmaschio, F. Davis, F. M. Shimizu, *Applied Surface Science Advances* **2021**, *6*, 100163.
[64] L. Xu, D. Li, S. Ramadan, Y. Li, N. Klein, *Biosens. Bioelectron.* **2020**, *170*, 112673.
[65] D. Shi, C. Zhang, X. Li, J. Yuan, *Biosens. Bioelectron.* **2023**, *220*, 10.1016/j.bios.2022.114898.
[66] R. Samson, G. R. Navale, M. S. Dharne, *3 Biotech* **2020**, *10*, 1–9.
[67] P. G. Jamkhande, N. W. Ghule, A. H. Bamer, M. G. Kalaskar, *J. Drug Delivery Sci. Technol.* **2019**, *53*, 10.1016/j.jddst.2019.101174.
[68] S. Iravani, H. Korbekandi, S. V. Mirmohammadi, B. Zolfaghari, *Synthesis of Silver Nanoparticles: Chemical, Physical and Biological Methods*, **2014**.
[69] S. Guo, E. Wang, *Anal. Chim. Acta* **2007**, *598*, 181–192.
[70] A. Gour, N. K. Jain, *Artif. Cells, Nanomed., Biotechnol.* **2019**, *47*, 844–851.
[71] D. K. Smith, B. A. Korgel, *Langmuir* **2008**, *24*, 644–649.
[72] S. E. Skrabalak, L. Au, X. Li, Y. Xia, *Nat. Protoc.* **2007**, *2*, 2182–2190.
[73] I. Ielo, G. Rando, F. Giacobello, S. Sfameni, A. Castellano, M. Galletta, D. Drommi, G. Rosace, M. R. Plutino, *Molecules* **2021**, *26*, 10.3390/molecules26195823.
[74] H. Duan, D. Wang, Y. Li, *Chem. Soc. Rev.* **2015**, *44*, 5778–5792.
[75] H. R. El-Seedi, R. M. El-Shabasy, S. A. M. Khalifa, A. Saeed, A. Shah, R. Shah, F. J. Iftikhar, M. M. Abdel-Daim, A. Omri, N. H. Hajrahand, J. S. M. Sabir, X. Zou, M. F. Halabi, W. Sarhan, W. Guo, *RSC Adv.* **2019**, *9*, 24539–24559.
[76] M. Schulz-Dobrick, K. V. Sarathy, M. Jansen, *J. Am. Chem. Soc.* **2005**, *127*, 12816–12817.
[77] A. Treshchalov, H. Erikson, L. Puust, S. Tsarenko, R. Saar, A. Vanetsev, K. Tammeveski, I. Sildos, *J. Colloid Interface Sci.* **2017**, *491*, 358–366.
[78] M. N. Nadagouda, T. F. Speth, R. S. Varma, *Acc. Chem. Res.* **2011**, *44*, 469–478.
[79] Z. Kereselidze, V. H. Romero, X. G. Peralta, F. Santamaria, *Journal of Visualized Experiments* **2012**, *59*, e3570.
[80] Z. Ren, H. Li, J. Li, J. Cai, L. Zhong, Y. Ma, Y. Pang, *Int. J. Biol. Macromol.* **2023**, *229*, 732–745.
[81] C. Jiang, J. Zhu, Z. Li, J. Luo, J. Wang, Y. Sun, *RSC Adv.* **2017**, *7*, 44463–44469.
[82] P. S. Pakchin, H. Ghanbari, R. Saber, Y. Omidi, *Biosens. Bioelectron.* **2018**, *122*, 68–74.
[83] A. Sánchez, A. Villalonga, G. Martínez-García, C. Parrado, R. Villalonga, *Nanomaterials* **2019**, *9*, 10.3390/nano9121745.
[84] B. Liu, M. Li, Y. Zhao, M. Pan, Y. Gu, W. Sheng, G. Fang, S. Wang, *Sensors (Switzerland)* **2018**, *18*, 10.3390/s18061946.
[85] M. Giannetto, L. Elviri, M. Careri, A. Mangia, G. Mori, *Biosens. Bioelectron.* **2010**, *26*, 2232–2236.
[86] X. Liu, D. Wang, Y. Li, *Nano Today* **2012**, *7*, 448–466.
[87] M. Kim, C. Lee, S. M. Ko, J. M. Nam, *J. Solid State Chem.* **2019**, *270*, 295–303.
[88] K. Loza, M. Heggen, M. Epple, *Adv. Funct. Mater.* **2020**, *30*, 10.1002/adfm.201909260.
[89] J. H. Park, H. S. Ahn, *Appl. Surf. Sci.* **2020**, *504*, 10.1016/j.apsusc.2019.144517.
[90] H. Kim, T. Y. Yoo, M. S. Bootharaju, J. H. Kim, D. Y. Chung, T. Hyeon, *Adv. Sci.* **2022**, *9*, 10.1002/advs.202104054.
[91] D. S. Idris, A. Roy, *Crystals (Basel)* **2023**, *13*, 10.3390/cryst13040637.
[92] R. Raghav, S. Srivastava, *Sens. Actuators B* **2015**, *220*, 557–564.
[93] X. Cao, N. Wang, S. Jia, L. Guo, K. Li, *Biosens. Bioelectron.* **2013**, *39*, 226–230.
[94] A. Kaur, S. Kapoor, A. Bharti, S. Rana, G. R. Chaudhary, N. Prabhakar, *J. Electroanal. Chem.* **2020**, *873*, 10.1016/j.jelechem.2020.114400.
[95] Y. Chen, A. J. Wang, P. X. Yuan, X. Luo, Y. Xue, J. J. Feng, *Biosens. Bioelectron.* **2019**, *132*, 294–301.

[96] M. Li, P. Wang, F. Pei, H. Yu, Y. Dong, Y. Li, Q. Liu, P. Chen, *Sens. Actuators B* **2018**, *261*, 22–30.
[97] M. Wu, Y. Yang, K. Cao, C. Zhao, X. Qiao, C. Hong, *Bioelectrochemistry* **2020**, *132*, 10.1016/j.bioelechem.2019.107434.
[98] Y. Chen, L.-P. Mei, J.-J. Feng, P.-X. Yuan, X. Luo, A.-J. Wang, *Biosens. Bioelectron.* **2019**, *145*, 111638.
[99] F. Li, Y. Li, J. Feng, Z. Gao, H. Lv, X. Ren, Q. Wei, *Biosens. Bioelectron.* **2018**, *100*, 512–518.
[100] N. Li, Y. Wang, Y. Li, W. Cao, H. Ma, D. Wu, B. Du, Q. Wei, *Sens. Actuators B* **2014**, *202*, 67–73.
[101] B. Jiang, C. Li, M. Imura, J. Tang, Y. Yamauchi, *Adv. Sci.* **2015**, *2*, 10.1002/advs.201500112.
[102] D. Philip, *Spectrochim Acta A Mol Biomol Spectrosc* **2009**, *73*, 374–381.
[103] D. Lomelí-Marroquín, D. M. Cruz, A. Nieto-Argüello, A. V. Crua, J. Chen, A. Torres-Castro, T. J. Webster, J. L. Cholula-Díaz, *Int. J. Nanomed.* **2019**, *14*, 2171–2190.
[104] A. Kumar, Y. Kuang, Z. Liang, X. Sun, *Mater. Today Nano* **2020**, *11*, 10.1016/j.mtnano.2020.100076.
[105] M. A. Farzin, H. Abdoos, *Talanta* **2021**, *224*, 10.1016/j.talanta.2020.121828.
[106] S. Chahal, J. R. Macairan, N. Yousefi, N. Tufenkji, R. Naccache, *RSC Adv.* **2021**, *11*, 25354–25363.
[107] Z. Zhang, Y. Cong, Y. Huang, X. Du, *Micromachines (Basel)* **2019**, *10*, 10.3390/mi10060397.
[108] C. Karaman, O. Karaman, N. Atar, Mehmet L. Yola, *Microchimica Acta* **2021**, *188*, 1–15, 10.1007/s00604-021-04838-6/Published.
[109] B. D. Mansuriya, Z. Altintas, *Materials* **2020**, *13*, 96.
[110] P. K. Gupta, D. Chauhan, Z. H. Khan, P. R. Solanki, *ACS Appl. Nano Mater.* **2020**, *3*, 2506–2516.
[111] E. Haque, J. Kim, V. Malgras, K. Raghava Reddy, A. C. Ward, J. You, Y. Bando, M. S. A. Hossain, Y. Yamauchi, *Small Methods* **2018**, *2*, 1–14.
[112] X. Liu, S. Zheng, Y. Hu, Z. Li, F. Luo, Z. He, *Food Anal. Methods* **2016**, *9*, 2972–2978.
[113] Z. Chen, B. Li, J. Liu, H. Li, C. Li, X. Xuan, M. Li, *Microchim. Acta* **2022**, *189*, 10.1007/s00604-022-05332-3.
[114] S. Zhang, H. Ma, L. Yan, W. Cao, T. Yan, Q. Wei, B. Du, *Biosens. Bioelectron.* **2014**, *59*, 335–341.
[115] Y. Wang, D. Fan, D. Wu, Y. Zhang, H. Ma, B. Du, Q. Wei, *Sens. Actuators B* **2016**, *236*, 241–248.
[116] L. Jiang, J. Han, F. Li, J. Gao, Y. Li, Y. Dong, Q. Wei, *Electrochim. Acta* **2015**, *160*, 7–14.
[117] M. P. Calatayud, C. Riggio, V. Raffa, B. Sanz, T. E. Torres, M. R. Ibarra, C. Hoskins, A. Cuschieri, L. Wang, J. Pinkernelle, G. Keilhoff, G. F. Goya, *J. Mater. Chem. B* **2013**, *1*, 3607–3616.
[118] J. Alonso, J. M. Barandiarán, L. Fernández Barquín, A. García-Arribas, *Magnetic Nanoparticles, Synthesis, Properties, and Applications*, **2018**.
[119] U. Tamer, Y. Gündoğdu, I. H. Boyaci, K. Pekmez, *J. Nanopart. Res.* **2010**, *12*, 1187–1196.
[120] Z. A. Lin, J. N. Zheng, F. Lin, L. Zhang, Z. Cai, G. N. Chen, *J. Mater. Chem.* **2011**, *21*, 518–524.
[121] M. E. Fleet, *Acta Crystallogr. Sect. B* **1981**, *37*, 917–920.
[122] D. Alcantara, L. Josephson, in *Frontiers of Nanoscience*, 4, Elsevier **2012**, 269–289, 10.1016/B978-0-12-415769-0.00011-X.
[123] S. Bhattacharya, in *Advances in Polymeric Nanomaterials for Biomedical Applications* (Eds.: A. K. Bajpai, R. K. Saini), Elsevier, **2021**, pp. 101–135.
[124] M. Freitas, H. P. A. Nouws, E. Keating, C. Delerue-Matos, *Sens. Actuators B* **2020**, *308*, 10.1016/j.snb.2020.127667.
[125] L. Fabiani, M. Saroglia, G. Galatà, R. De Santis, S. Fillo, V. Luca, G. Faggioni, N. D'Amore, E. Regalbuto, P. Salvatori, G. Terova, D. Moscone, F. Lista, F. Arduini, *Biosens. Bioelectron.* **2021**, *171*, 10.1016/j.bios.2020.112686.
[126] V. Poulichet, M. Morel, S. Rudiuk, D. Baigl, *Journal of Colloid and Interface Science* **2020**, *573*, 370–375.
[127] L. T. Tufa, S. Oh, V. T. Tran, J. Kim, K. J. Jeong, T. J. Park, H. J. Kim, J. Lee, *Electrochim. Acta* **2018**, *290*, 369–377.
[128] S. Wei, H. Xiao, L. Cao, Z. Chen, *Biosensors (Basel)* **2020**, *10*, 10.3390/bios10030024.
[129] H. Ehzari, M. Samimi, M. Safari, M. B. Gholivand, *J. Electroanal. Chem.* **2020**, *877*, 10.1016/j.jelechem.2020.114722.
[130] J. Huang, T. Zhou, W. Zhao, M. Zhang, Z. Zhang, W. Lai, N. R. Kadasala, H. Liu, Y. Liu, *Nanomaterials* **2022**, *12*, 10.3390/nano12193322.
[131] A. Shamsazar, A. Asadi, D. Seifzadeh, M. Mahdavi, *Sens. Actuators B* **2021**, *346*, 10.1016/j.snb.2021.130459.
[132] P. G. Rudakovskaya, E. K. Beloglazkina, A. G. Majouga, N. L. Klyachko, A. v Kabanov, N. v Zyk, *Moscow Univ. Chem. Bull.* **2015**, *70*, 149–156.
[133] M. S. A. Darwish, H. Kim, H. Lee, C. Ryu, J. Y. Lee, J. Yoon, *Nanomaterials* **2020**, *10*, 1–16.
[134] I. Robinson, L. D. Tung, S. Maenosono, C. Wälti, N. T. K. Thanh, *Nanoscale* **2010**, *2*, 2624–2630.
[135] L. Wang, H.-Y. Park, I. Stephanie, I. Lim, M. J. Schadt, D. Mott, J. Luo, X. Wang, C.-J. Zhong, *J. Mater. Chem.* **2008**, *18*, 2629–2635.
[136] R. Zumpano, F. Polli, C. D. Agostino, R. Antiochia, G. Favero, F. Mazzei, *Electrochemistry* **2021**, *2*, 10–28.
[137] A. A. El-Gendy, *Core/Shell Magnetic Nanoparticles for Biomedical Applications*, Elsevier Inc., **2018**.
[138] F. Polli, C. D'Agostino, R. Zumpano, V. de Martino, G. Favero, L. Colangelo, S. Minisola, F. Mazzei, *Talanta* **2023**, *251*, 10.1016/j.talanta.2022.123755.
[139] A. Ahmadi, H. Shirazi, N. Pourbagher, A. Akbarzadeh, K. Omidfar, *Mol. Biol. Rep.* **2014**, *41*, 1659–1668.
[140] B. Piro, S. Reisberg, *Sensors (Switzerland)* **2017**, *17*, 10.3390/s17040794.
[141] G. Bergström, C. F. Mandenius, *Sens. Actuators B* **2011**, *158*, 265–270.
[142] F. Duval, T. A. van Beek, H. Zuilhof, *Analyst* **2015**, *140*, 6467–6472.
[143] Y. Jung, J. M. Lee, H. Jung, B. H. Chung, *Anal. Chem.* **2007**, *79*, 6534–6541.
[144] J. Baniukevic, J. Kirlyte, A. Ramanavicius, A. Ramanaviciene, *Procedia Eng.* **2012**, *47*, 837–840.
[145] J. Buijs, J. W. T. Lichtenbelt, W. Norde, J. Lyklema, *Colloids. Surf. B Biointerfaces* **1995**, *5*, 11–23.
[146] Y. Liu, J. Yu, *Microchim. Acta* **2016**, *183*, 1–19.
[147] M. E. Wiseman, C. W. Frank, *Langmuir* **2012**, *28*, 1765–1774.
[148] D. Quaglio, F. Polli, C. del Plato, G. Cianfoni, C. Tortora, F. Mazzei, B. Botta, A. Calcaterra, F. Ghirga, *Supramol. Chem.* **2021**, *33*, 1–25.
[149] D. Quaglio, L. Mangiardi, G. Venditti, C. del Plato, F. Polli, F. Ghirga, G. Favero, M. Pierini, B. Botta, F. Mazzei, *Chem. Eur. J.* **2020**, *26*, 8400–8406.
[150] E. Capecchi, D. Piccinino, E. Tomaino, B. M. Bizzarri, F. Polli, R. Antiochia, F. Mazzei, R. Saladino, *RSC Adv.* **2020**, *10*, 29031–29042.
[151] V. L. Dhadge, A. Hussain, A. M. Azevedo, R. Aires-Barros, A. C. A. Roque, *J. R. Soc. Interface* **2014**, *11*, 10.1098/rsif.2013.0875.
[152] S. K. Vashist, J. H. T. Luong, *Handbook of Immunoassay Technologies* **2018**, 1–18.
[153] C. Chen, W. Liu, T. Hong, *Analyst* **2019**, *144*, 3912–3924.
[154] P. Peluso, D. S. Wilson, D. Do, H. Tran, M. Venkatasubbaiah, D. Quincy, B. Heidecker, K. Poindexter, N. Tolani, M. Phelan, K. Witte, L. S. Jung, P. Wagner, S. Nock, *Anal. Biochem.* **2003**, *312*, 113–124.
[155] K. Gajos, P. Petrou, A. Budkowski, *Molecules* **2022**, *27*, 10.3390/molecules27123672.
[156] S. Chen, L. Liu, J. Zhou, S. Jiang, *Langmuir* **2003**, *19*, 2859–2864.
[157] J. Zhou, H. K. Tsao, Y. J. Sheng, S. Jiang, *J. Chem. Phys.* **2004**, *121*, 1050–1057.
[158] A. J. Sivaram, A. Wardiana, C. B. Howard, S. M. Mahler, K. J. Thurecht, *Adv. Healthcare Mater.* **2018**, *7*, 1700607.
[159] R. Franco, E. Pereira, *Encyclopedia of Metalloproteins* **2013**, 908–915, 10.1007/978-1-4614-1533-6_572.
[160] D. Lou, L. Ji, L. Fan, Y. Ji, N. Gu, Y. Zhang, *Langmuir* **2019**, *35*, 4860–4867.
[161] S. Gao, J. M. Guisán, J. Rocha-Martin, *Anal. Chim. Acta* **2022**, *1189*, 10.1016/j.aca.2021.338907.
[162] R. Terracciano, A. Zhang, E. B. Butler, D. Demarchi, J. H. Hafner, A. Grattoni, C. S. Filgueira, *Pharmaceutica* **2021**, *13*, 216.
[163] K. Zhang, Z. Cao, S. Wang, J. Chen, Y. Wei, D. Feng, *Int. J. Electrochem. Sci.* **2020**, *15*, 2604–2613.
[164] S. Wignarajah, I. Chianella, I. E. Tothill, *Biosensors (Basel)* **2023**, *13*, 355.
[165] L. Zhang, Y. Mazouzi, M. Salmain, B. Liedberg, S. Boujday, *Biosens. Bioelectron.* **2020**, *165*, 10.1016/j.bios.2020.112370.
[166] M. Freitas, A. Carvalho, H. P. A. Nouws, C. Delerue-Matos, *Biosensors (Basel)* **2022**, *12*, 10.3390/bios12060429.
[167] C. M. Silveira, R. Zumpano, M. Moreira, M. P. de Almeida, M. J. Oliveira, M. Bento, C. Montez, I. Paixão, R. Franco, E. Pereira, M. G. Almeida, *ChemElectroChem* **2019**, *6*, 4696–4703.
[168] A. Domínguez-Aragón, E. A. Zaragoza-Contreras, G. Figueroa-Miranda, A. Offenhäusser, D. Mayer, *Biosensors (Basel)* **2022**, *13*, 63.
[169] P. Hloma, G. E. Uwaya, K. Bisetty, *Biosens. Bioelectron.* **2022**, *11*, 100203.
[170] K. S. Prasad, X. Cao, N. Gao, Q. Jin, S. T. Sanjay, G. Henao-Pabon, X. J. Li, *Sens. Actuators B* **2020**, *305*, 127516.
[171] N. E. Pollok, C. Rabin, C. T. Walgama, L. Smith, I. Richards, R. M. Crooks, *ACS Sens.* **2020**, *5*, 853–860.
[172] A. Roberts, S. Mahari, S. Gandhi, *J. Electroanal. Chem.* **2022**, *919*, 116563.

[173] S. Khan, Akrema, S. Qazi, R. Ahmad, K. Raza, Rahisuddin, *ACS Omega* **2021**, *6*, 16076–16085.
[174] M. J. E. Fischer, in *Surface Plasmon Resonance: Methods and Protocols* (Eds.: N. J. Mol, M. J. E. Fischer), Humana Press, Totowa, NJ, **2010**, pp. 55–73.
[175] R. E. Ducker, M. T. Montague, G. J. Leggett, *Biointerphases* **2008**, *3*, 59–65.
[176] F. López-Gallego, L. Betancor, C. Mateo, A. Hidalgo, N. Alonso-Morales, G. Dellamora-Ortiz, J. M. Guisán, R. Fernández-Lafuente, *J. Biotechnol.* **2005**, *119*, 70–75.
[177] I. Migneault, C. Dartiguenave, M. J. Bertrand, K. C. Waldron, *BioTechniques* **2004**, *37*, 790–802.
[178] L. Betancor, F. López-Gallego, N. Alonso-Morales, G. Dellamora, C. Mateo, R. Fernandez-Lafuente, J. M. Guisan, *Glutaraldehyde in Protein Immobilization A Versatile Reagent*, **n.d.**
[179] Y. Wine, N. Cohen-Hadar, A. Freeman, F. Frolow, *Biotechnol. Bioeng.* **2007**, *98*, 711–718.
[180] V. Crivianu-Gaita, M. Thompson, *Biosens. Bioelectron.* **2015**, *70*, 167–180.
[181] B. Y. Kim, C. B. Swearingen, J. A. Ho, E. V. Romanova, P. W. Bohn, J. V. Sweedler, *J. Am. Chem. Soc.* **2007**, *129*, 7620–7626.
[182] G. N. Fadhilah, M. Yusuf, A. K. Sari, T. R. Tohari, H. L. Wiraswati, S. Ekawardhani, L. Faridah, N. Fauziah, I. Anshori, Y. Wahyuni Hartati, *ChemistrySelect* **2023**, *8*, 10.1002/slct.202203928.
[183] K. Tsugimura, H. Ohnuki, H. Wu, H. Endo, D. Tsuya, M. Izumi, *J. Phys. Conf. Ser.* **2017**, *924*, 10.1088/1742-6596/924/1/012015.
[184] S. Kossek, C. Padeste, L. Tiefenauer, *J. Mol. Recognit.* **1996**, *9*, 485–487.
[185] S. Akbari Nakhjavani, B. Khalilzadeh, H. Afsharan, N. Hosseini, M. H. Ghahremani, S. Carrara, S. Tasoglu, Y. Omidi, *Microchim. Acta* **2023**, *190*, 10.1007/s00604-023-05656-8.
[186] Y. Lee, E. K. Lee, Y. W. Cho, T. Matsui, I. C. Kang, T. S. Kim, M. H. Han, *Proteomics* **2003**, *3*, 2289–2304.
[187] H. Chen, F. Liu, F. Qi, K. Koh, K. Wang, *Int. J. Mol. Sci.* **2014**, *15*, 5496–5507.
[188] S. Emaminejad, M. Javanmard, C. Gupta, S. Chang, R. W. Davis, R. T. Howe, *Proc. Natl. Acad. Sci. USA* **2015**, *112*, 1995–1999.
[189] L. Mutihac, J. H. Lee, J. S. Kim, J. Vicens, *Chem. Soc. Rev.* **2011**, *40*, 2777–2796.
[190] H. Chen, J. Huang, J. Lee, S. Hwang, K. Koh, *Sens. Actuators B* **2010**, *147*, 548–553.
[191] M. Soler, M. C. Estevez, M. Alvarez, M. A. Otte, B. Sepulveda, L. M. Lechuga, *Sensors (Switzerland)* **2014**, *14*, 2239–2258.
[192] A. Wei, *Chem. Commun.* **2006**, 1581–1591.
[193] J. M. Ha, A. Solovyov, A. Katz, *Langmuir* **2009**, *25*, 10548–10553.
[194] A. Amiri, E. Y. Choi, H. J. Kim, *J. Inclusion Phenom. Macrocyclic Chem.* **2010**, *66*, 185–194.
[195] R. Kumar, A. Sharma, H. Singh, P. Suating, H. S. Kim, K. Sunwoo, I. Shim, B. C. Gibb, J. S. Kim, *Chem. Rev.* **2019**, *119*, 9657–9721.
[196] A. R. Kongor, V. A. Mehta, K. M. Modi, M. K. Panchal, S. A. Dey, U. S. Panchal, V. K. Jain, *Top. Curr. Chem.* **2016**, *374*, 10.1007/s41061-016-0029-z.
[197] N. Verma, P. Sutariya, T. Patel, M. Shukla, A. Pandya, *Biomed. Microdevices* **2023**, *25*, 10.1007/s10544-022-00640-0.
[198] M. Retout, P. Blond, I. Jabin, G. Bruylants, *Bioconjugate Chem.* **2021**, *32*, 290–300.
[199] F. Polli, G. Cianfoni, R. Elnahas, L. Mangiardi, F. A. Scaramuzzo, S. Cammarone, D. Quaglio, A. Calcaterra, M. Pierini, F. Mazzei, R. Zanoni, B. Botta, F. Ghirga, *ChemBioChem* **2023**, *24*, 10.1002/cbic.202300030.
[200] A. Calcaterra, F. Polli, L. Lamelza, C. Del Plato, S. Cammarone, F. Ghirga, B. Botta, F. Mazzei, D. Quaglio, *Bioconjugate Chem.* **2023**, *34*, 529–537.
[201] R. Zumpano, M. Manghisi, F. Polli, C. D'Agostino, F. Ietto, G. Favero, F. Mazzei, *Anal. Bioanal. Chem.* **2022**, 10.1007/s00216-021-03838-y.
[202] A. Makaraviciute, A. Ramanaviciene, *Biosens. Bioelectron.* **2013**, *50*, 460–471.
[203] M. Page, R. Thorpe, in *The Protein Protocols Handbook*, Springer, **2002**, pp. 993–994.
[204] Y. Khaniani, Y. Ma, M. Ghadiri, J. Zeng, D. Wishart, S. Babiuk, C. Charlton, J. N. Kanji, J. Chen, *Sci. Rep.* **2022**, *12*, 10.1038/s41598-022-17219-7.
[205] X. Wang, N. Xia, L. Liu, *Int. J. Mol. Sci.* **2013**, *14*, 20890–20912.
[206] P. Hashemi, A. Afkhami, B. Baradaran, R. Halabian, T. Madrakian, F. Arduini, T. A. Nguyen, H. Bagheri, *Anal. Chem.* **2020**, *92*, 11405–11412.
[207] C. D'Agostino, C. Chillocci, F. Polli, L. Surace, F. Simonetti, M. Agostini, S. Brutti, F. Mazzei, G. Favero, R. Zumpano, *Molecules* **2023**, *28*, 5425.
[208] M. Serhan, M. Sprowls, D. Jackemeyer, M. Long, I. D. Perez, W. Maret, N. Tao, E. Forzani, *AIChE Annual Meeting, Conference Proceedings* **2019**, 10.1039/x0xx00000x.
[209] W. Wen, X. Yan, C. Zhu, D. Du, Y. Lin, *Anal. Chem.* **2017**, *89*, 138–156.
[210] P. Fanjul-Bolado, M. B. González-García, A. Costa-García, *Anal. Bioanal. Chem.* **2005**, *382*, 297–302.
[211] A. Erdem, H. Senturk, E. Yildiz, M. Maral, *Talanta* **2022**, *244*, 10.1016/j.talanta.2022.123422.
[212] C. Shen, L. Wang, H. Zhang, S. Liu, J. Jiang, *Front. Chem.* **2020**, *8*, 10.3389/fchem.2020.589560.
[213] A. Jing, Q. Xu, W. Feng, G. Liang, *Micromachines (Basel)* **2020**, *11*, 10.3390/mi11070660.
[214] P. Chen, X. Hua, J. Liu, H. Liu, F. Xia, D. Tian, C. Zhou, *Anal. Biochem.* **2019**, *574*, 23–30.
[215] T. Monteiro, R. Zumpano, C. M. Silveira, M. Gabriela Almeida, *Enzymes for Solving Humankind's Problems: Natural and Artificial Systems in Health, Agriculture, Environment and Energy* **2021**, 303–362, 10.1007/978-3-030-58315-6_11.
[216] L. Ciogli, R. Zumpano, A. A. Poloznikov, D. M. Hushpulian, V. I. Tishkov, R. Andreu, L. Gorton, F. Mazzei, G. Favero, P. Bollella, *ChemElectroChem* **2021**, *8*, 2495–2504.
[217] Y. Liu, G. He, H. Liu, H. Yin, F. Gao, J. Chen, S. Zhang, B. Yang, *RSC Adv.* **2020**, *10*, 7912–7917.
[218] H. Ding, L. Yang, H. Jia, D. Fan, Y. Zhang, X. Sun, Q. Wei, H. Ju, *Sens. Actuators B* **2020**, *312*, 10.1016/j.snb.2020.127980.
[219] Z. Gao, Y. Li, C. Zhang, S. Zhang, F. Li, P. Wang, H. Wang, Q. Wei, *Biosens. Bioelectron.* **2019**, *126*, 108–114.
[220] Y. Huang, F. Zhu, J. Guan, W. Wei, L. Zou, *Biosensors (Basel)* **2021**, *11*, 10.3390/bios11010005.
[221] L. Dai, Y. Li, Y. Wang, X. Luo, D. Wei, R. Feng, T. Yan, X. Ren, B. Du, Q. Wei, *Biosens. Bioelectron.* **2019**, *132*, 97–104.
[222] G. Lai, F. Yan, J. Wu, C. Leng, H. Ju, *Anal. Chem.* **2011**, *83*, 2726–2732.
[223] G. Lai, J. Wu, H. Ju, F. Yan, *Adv. Funct. Mater.* **2011**, *21*, 2938–2943.
[224] D. Lin, J. Wu, M. Wang, F. Yan, H. Ju, *Anal. Chem.* **2012**, *84*, 3662–3668.
[225] D. Lin, J. Wu, H. Ju, F. Yan, *Biosens. Bioelectron.* **2013**, *45*, 195–200.
[226] Z. Štukovnik, U. Bren, *Int. J. Mol. Sci.* **2022**, *23*, 15922.
[227] C. Robinson, V. B. Juska, A. O'Riordan, **2022**.
[228] M. Nemati, M. A. Farajzadeh, M. R. Afshar Mogaddam, A. Pourali, *Crit. Rev. Anal. Chem.* **2022**, *0*, 1–14.
[229] S. Rana, A. Bharti, S. Singh, A. Bhatnagar, N. Prabhakar, *Microchim. Acta* **2020**, *187*, 10.1007/s00604-020-04599-8.
[230] V. S. Kumar, S. Kummari, G. Catanante, K. V. Gobi, J. L. Marty, K. Y. Goud, *Sens. Actuators B* **2023**, *377*, 10.1016/j.snb.2022.133077.
[231] A. L. Lorenzen, A. M. dos Santos, L. P. dos Santos, L. da Silva Pinto, F. R. Conceição, F. Wolfart, *Electrochim. Acta* **2022**, *404*, 10.1016/j.electacta.2021.139757.
[232] E. B. Aydın, M. Aydın, M. K. Sezgintürk, *Sens. Actuators B* **2022**, *367*, 10.1016/j.snb.2022.132099.
[233] Z. You, Q. Qiu, H. Chen, Y. Feng, X. Wang, Y. Wang, Y. Ying, *Biosens. Bioelectron.* **2020**, *150*, 10.1016/j.bios.2019.111896.
[234] R. P. Ojha, P. Singh, U. P. Azad, R. Prakash, *Electrochim. Acta* **2022**, *411*, 10.1016/j.electacta.2022.140069.
[235] G. Ibáñez-Redín, R. H. M. Furuta, D. Wilson, F. M. Shimizu, E. M. Materon, L. M. R. B. Arantes, M. E. Melendez, A. L. Carvalho, R. M. Reis, M. N. Chaur, D. Gonçalves, O. N. Oliveira, *Mater. Sci. Eng. C* **2019**, *99*, 1502–1508.
[236] F. Silveri, R. Oboňilová, J. Máčala, D. Compagnone, P. Skládal, *Microchim. Acta* **2023**, *190*, 306.
[237] T. Dahiya, Ravina, A. Mann, H. Mohan, M. Sharma, C. S. Pundir, J. S. Rana, *J. Mater. Sci.* **2023**, *58*, 4739–4752.
[238] A. Kirchhain, A. Bonini, F. Vivaldi, N. Poma, F. Di Francesco, *TrAC Trends Anal. Chem.* **2020**, *133*, 116073.
[239] N. Tasić, L. Cavalcante, E. Deffune, M. S. Góes, T. R. L. C. Paixão, L. M. Gonçalves, *Electrochim. Acta* **2021**, *397*, 10.1016/j.electacta.2021.139244.
[240] B. Chen, J. Kiely, I. Williams, R. Luxton, *Bioelectrochemistry* **2023**, *153*, 10.1016/j.bioelechem.2023.108456.
[241] P. Bergveld, *IEEE Trans. Biomed. Eng.* **1970**, 70–71.
[242] E. S. Zachariah, P. Gopalakrishnakone, P. Neuzil, in *Encyclopedia of Medical Devices and Instrumentation*, Wiley, **2006**.
[243] G. Gifta, D. G. N. Rani, *ECS J. Solid State Sci. Technol.* **2020**, *9*, 121005.
[244] T. Wadhera, D. Kakkar, G. Wadhwa, B. Raj, *J. Electron. Mater.* **2019**, *48*, 7635–7646.
[245] B. L. Allen, P. D. Kichambare, A. Star, *Adv. Mater.* **2007**, *19*, 1439–1451.

[246] M. T. Amen, T. T. T. Pham, E. Cheah, D. P. Tran, B. Thierry, *Molecules* **2022**, *27*, 7952.
[247] T. Manimekala, R. Sivasubramanian, G. Dharmalingam, *J. Electron. Mater.* **2022**, *51*, 1950–1973.
[248] S. S. Siti, S. Nadzirah, J. Kazmi, R. A. Rahim, C. F. Dee, A. A. Hamzah, M. A. Mohamed, *J. Mater. Sci.* **2021**, *56*, 15344–15353.
[249] M. S. Krishna, S. Singh, M. Batool, H. M. Fahmy, K. Seku, A. E. Shalan, S. Lanceros-Mendez, M. N. Zafar, *Mater Adv* **2022**, 320–354.
[250] H. Rahmani, S. Mansouri Majd, A. Salimi, F. Ghasemi, *Talanta* **2023**, *257*, 124336.
[251] S. Ramadan, R. Lobo, Y. Zhang, L. Xu, O. Shaforost, D. K. H. Tsang, J. Feng, T. Yin, M. Qiao, A. Rajeshirke, L. R. Jiao, P. K. Petrov, I. E. Dunlop, M. M. Titirici, N. Klein, *ACS Appl. Mater. Interfaces* **2021**, *13*, 7854–7864.
[252] C. A. Vu, W. Y. Chen, Y. S. Yang, H. W. H. Chan, *Sens. Actuators B* **2021**, *329*, 129150.
[253] G. Rabbani, M. E. Khan, E. Ahmad, M. V. Khan, A. Ahmad, A. U. Khan, W. Ali, M. A. Zamzami, A. H. Bashiri, W. Zakri, *Bioelectrochemistry* **2023**, 108493.
[254] D. Lee, J. Bhardwaj, J. Jang, *Sci. Rep.* **2022**, *12*, 10.1038/s41598-022-06101-1.
[255] D. Shi, C. Zhang, X. Li, J. Yuan, *Biosens. Bioelectron.* **2023**, *220*, 10.1016/j.bios.2022.114898.
[256] X. Ruan, Y. Wang, E. Y. Kwon, L. Wang, N. Cheng, X. Niu, S. Ding, B. J. Van Wie, Y. Lin, D. Du, *Biosens. Bioelectron.* **2021**, *184*, 10.1016/j.bios.2021.113238.
[257] Z. Du, Y. Wang, D. He, E. Xu, Q. Chai, Z. Jin, Z. Wu, B. Cui, *Food Chem.* **2022**, *397*, 10.1016/j.foodchem.2022.133756.
[258] L. Yin, T. You, H. R. El-Seedi, I. M. El-Garawani, Z. Guo, X. Zou, J. Cai, *Food Chem.* **2022**, *396*, 10.1016/j.foodchem.2022.133707.
[259] J. Wang, Q. Yang, H. Liu, Y. Chen, W. Jiang, Y. Wang, H. Zeng, *Food Chem.* **2022**, *378*, 10.1016/j.foodchem.2022.132112.
[260] M. A. Ali, C. Hu, F. Zhang, S. Jahan, B. Yuan, M. S. Saleh, S. J. Gao, R. Panat, *J. Med. Virol.* **2022**, *94*, 10.1002/jmv.27591.
[261] L. Wang, W. Gao, S. Ng, M. Pumera, *Anal. Chem.* **2021**, *93*, 10.1021/acs.analchem.1c00322.
[262] D. Jiang, K. Sheng, H. Jiang, L. Wang, *Bioelectrochemistry* **2021**, *142*, 10.1016/j.bioelechem.2021.107919.
[263] T. Laochai, J. Yukird, N. Promphet, J. Qin, O. Chailapakul, N. Rodthongkum, *Biosens. Bioelectron.* **2022**, *203*, 10.1016/j.bios.2022.114039.
[264] L. Tian, M. Jiang, M. Su, X. Cao, Q. Jiang, Q. Liu, C. Yu, *Microchem. J.* **2023**, *185*, 10.1016/j.microc.2022.108172.
[265] M. A. Mujawar, H. Gohel, S. K. Bhardwaj, S. Srinivasan, N. Hickman, A. Kaushik, *Mater. Today Chem.* **2020**, *17*, 10.1016/j.mtchem.2020.100306.
[266] C. Huang, J. Wang, S. Wang, Y. Zhang, *Neurocomputing* **2023**, *557*, 10.1016/j.neucom.2023.126719.
[267] S. Jain, M. Nehra, R. Kumar, N. Dilbaghi, T. Y. Hu, S. Kumar, A. Kaushik, C. zhong Li, *Biosens. Bioelectron.* **2021**, *179*, 10.1016/j.bios.2021.113074.
[268] P. Manickam, S. A. Mariappan, S. M. Murugesan, S. Hansda, A. Kaushik, R. Shinde, S. P. Thipperudraswamy, *Biosensors (Basel)* **2022**, *12*, 10.3390/bios12080562.
[269] S. Fortunati, C. Giliberti, M. Giannetto, A. Bolchi, D. Ferrari, G. Donofrio, V. Bianchi, A. Boni, I. De Munari, M. Careri, *Biosensors (Basel)* **2022**, *12*, 10.3390/bios12060426.
[270] L. Du, Y. Yan, T. Li, H. Liu, N. Li, X. Wang, *ACS ES and T Engineering* **2022**, *2*, 92–100.
[271] J. Song, V. Pandian, M. G. Mauk, H. H. Bau, S. Cherry, L. C. Tisi, C. Liu, *Anal. Chem.* **2018**, *90*, 4823–4831.
[272] X. Lu, P. Liu, K. Bisetty, Y. Cai, X. Duan, Y. Wen, Y. Zhu, L. Rao, Q. Xu, J. Xu, *J. Electroanal. Chem.* **2022**, *920*, 10.1016/j.jelechem.2022.116634.
[273] Y. Wang, Y. Wang, D. Wu, H. Ma, Y. Zhang, D. Fan, X. Pang, B. Du, Q. Wei, *Sens. Actuators B* **2018**, *255*, 125–132.
[274] M. Rizwan, S. Elma, S. A. Lim, M. U. Ahmed, *Biosens. Bioelectron.* **2018**, *107*, 211–217.
[275] Q. Yan, Y. Yang, Z. Tan, Q. Liu, H. Liu, P. Wang, L. Chen, D. Zhang, Y. Li, Y. Dong, *Biosens. Bioelectron.* **2018**, *103*, 151–157.
[276] S. C. Barman, M. F. Hossain, H. Yoon, J. Y. Park, *Biosens. Bioelectron.* **2018**, *100*, 16–22.
[277] Y. Yang, Q. Yan, Q. Liu, Y. Li, H. Liu, P. Wang, L. Chen, D. Zhang, Y. Li, Y. Dong, *Biosens. Bioelectron.* **2018**, *99*, 450–457.
[278] Y. Wang, G. Zhao, Y. Zhang, X. Pang, W. Cao, B. Du, Q. Wei, *Sens. Actuators B* **2018**, *266*, 561–569.
[279] Z. Tang, J. He, J. Chen, Y. Niu, Y. Zhao, Y. Zhang, C. Yu, *Biosens. Bioelectron.* **2018**, *101*, 253–259.
[280] M. Mathelié-Guinlet, T. Cohen-Bouhacina, I. Gammoudi, A. Martin, L. Béven, M. H. Delville, C. Grauby-Heywang, *Sens. Actuators B* **2019**, *292*, 314–320.
[281] D. Sun, H. Li, M. Li, C. Li, L. Qian, B. Yang, *Biosens. Bioelectron.* **2019**, *132*, 68–75.
[282] R. Devi, S. Gogoi, S. Barua, H. Sankar Dutta, M. Bordoloi, R. Khan, *Food Chem.* **2019**, *276*, 350–357.
[283] Y. Chen, L. P. Mei, J. J. Feng, P. X. Yuan, X. Luo, A. J. Wang, *Biosens. Bioelectron.* **2019**, *145*, 10.1016/j.bios.2019.111638.
[284] M. Hu, X. Hu, Y. Zhang, M. Teng, R. Deng, G. Xing, J. Tao, G. Xu, J. Chen, Y. Zhang, G. Zhang, *Sens. Actuators B* **2019**, *288*, 571–578.
[285] H. Medetalibeyoglu, G. Kotan, N. Atar, M. L. Yola, *Talanta* **2020**, *220*, 10.1016/j.talanta.2020.121403.
[286] Q. Lan, C. Ren, A. Lambert, G. Zhang, J. Li, Q. Cheng, X. Hu, Z. Yang, *ACS Sustainable Chem. Eng.* **2020**, *8*, 4392–4399.
[287] A. Roberts, S. Mahari, D. Shahdeo, S. Gandhi, *Anal. Chim. Acta* **2021**, *1188*, 339207.
[288] N. Chaudhary, A. K. Yadav, J. G. Sharma, P. R. Solanki, *J. Environ. Chem. Eng.* **2021**, *9*, 106771.
[289] Y. Wang, P. Wang, Z. Zhao, S. Ye, W. Wang, Q. Liu, Y. Li, D. Zhang, Y. Li, *Bioelectrochemistry* **2023**, *152*, 108405.
[290] R. Zumpano, M. Manghisi, F. Polli, C. D'Agostino, F. Ietto, G. Favero, F. Mazzei, *Anal. Bioanal. Chem.* **2022**, *414*, 2055–2064.
[291] M. A. Sadique, S. Yadav, V. Khare, R. Khan, G. K. Tripathi, P. S. Khare, *Diagnostik* **2022**, *12*, 10.3390/diagnostics12112612.
[292] A. Kumar, T. Sarkar, P. R. Solanki, *Biosensors (Basel)* **2023**, *13*, 10.3390/bios13020177.
[293] T. R. de Oliveira, D. H. Martucci, R. C. Faria, *Sens. Actuators B* **2018**, *255*, 684–691.
[294] Y. Khristunova, E. Korotkova, B. Kratochvil, J. Barek, E. Dorozhko, V. Vyskocil, E. Plotnikov, O. Voronova, V. Sidelnikov, *Sensors (Switzerland)* **2019**, *19*, 10.3390/s19092103.
[295] C. Zhang, S. Zhang, Y. Jia, Y. Li, P. Wang, Q. Liu, Z. Xu, X. Li, Y. Dong, *Biosens. Bioelectron.* **2019**, *126*, 785–791.
[296] X. Zhang, Y. Li, H. Lv, J. Feng, Z. Gao, P. Wang, Y. Dong, Q. Liu, Z. Zhao, *Biosens. Bioelectron.* **2018**, *106*, 142–148.
[297] H. Lv, Y. Li, X. Zhang, Z. Gao, C. Zhang, S. Zhang, Y. Dong, *Biosens. Bioelectron.* **2018**, *112*, 1–7.
[298] F. Pei, P. Wang, E. Ma, H. Yu, C. Gao, H. Yin, Y. Li, Q. Liu, Y. Dong, *Biosens. Bioelectron.* **2018**, *122*, 231–238.
[299] M. Li, P. Wang, F. Pei, H. Yu, Y. Dong, Y. Li, Q. Liu, P. Chen, *Sens. Actuators B* **2018**, *261*, 22–30.
[300] D. Quesada-González, A. Baiocco, A. A. Martos, A. de la Escosura-Muñiz, G. Palleschi, A. Merkoçi, *Biosens. Bioelectron.* **2019**, *127*, 150–154.
[301] T. Zhang, B. Xing, Q. Han, Y. Lei, D. Wu, X. Ren, Q. Wei, *Anal. Chim. Acta* **2018**, *1032*, 10.1016/j.aca.2018.05.035.
[302] Z. Rahmati, M. Roushani, H. Hosseini, H. Choobin, *Microchem. J.* **2021**, *170*, 10.1016/j.microc.2021.106718.

Manuscript received: August 14, 2023
Revised manuscript received: November 12, 2023
Version of record online: ■■, ■■

REVIEW

Nanoparticle-based electrochemical immunosensors are fascinating and promising screening systems that rely on the specific affinity binding between antibodies and antigens. In this review, we summarize recent advancements in the use of nanoparticles for realizing highly sensitive and biocompatible electrochemical immunosensors, mainly focusing on design, fabrication, and applications and discussing the remaining challenges and future perspectives.

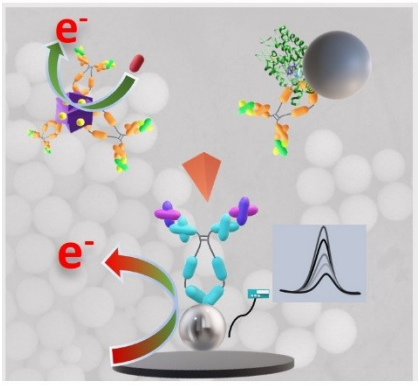

Dr. F. Polli, F. Simonetti, L. Surace, Dr. M. Agostini, Prof. G. Favero, Prof. F. Mazzei, Dr. R. Zumpano**